

## ULTRASTRUCTURE AND LSU rDNA-BASED REVISION OF *PERIDINIUM* GROUP PALATINUM (DINOPHYCEAE) WITH THE DESCRIPTION OF *PALATINUS* GEN. NOV.<sup>1</sup>

Sandra C. Craveiro, António J. Calado<sup>2</sup>

GeoBioSciences, GeoTechnologies and GeoEngineering (GeoBioTec) Research Unit and Departamento de Biologia, Universidade de Aveiro, P-3810-193 Aveiro, Portugal

Niels Daugbjerg and Øyvind Moestrup

Phycology Laboratory, Department of Biology, University of Copenhagen, Øster Farimagsgade 2D, DK-1353 Copenhagen K, Denmark

The name *Peridinium palatinum* Lauterborn currently designates a freshwater peridinioid with 13 epithelial and six cingular plates, and no apical pore complex. Freshwater dinoflagellate floras classify it in *Peridinium* group palatinum together with *P. pseudolaeve* M. Lefèvre. General ultrastructure, flagellar apparatus, and pusular components of *P. palatinum* were examined by serial section TEM and compared to *P. cinctum* (O. F. Müll.) Ehrenb. and *Peridiniopsis borgei* Lemmerm., respectively, types of *Peridinium* and *Peridiniopsis*. Partial LSU rDNA sequences from *P. palatinum*, *P. pseudolaeve* and several peridinioids, woloszynskioids, gymnodioids, and other dinoflagellates were used for a phylogenetic analysis. General morphology and tabulation of taxa in group palatinum were characterized by SEM. Differences in plate numbers, affecting both the epitheca and the cingulum, combine with differences in plate ornamentation and a suite of internal cell features to suggest a generic-level distinction between *Peridinium* group palatinum and typical *Peridinium*. The branching pattern of the phylogenetic tree is compatible with this conclusion, although with low support from bootstrap values and posterior probabilities, as are sequence divergences estimated between species in group palatinum, and typical *Peridinium* and *Peridiniopsis*. *Palatinus* nov. gen. is proposed with the new combinations *Palatinus apiculatus* nov. comb. (type species; syn. *Peridinium palatinum*), *P. apiculatus* var. *laevis* nov. comb., and *P. pseudolaevis* nov. comb. Distinctive characters for *Palatinus* include a smooth or slightly granulate, but not areolate, plate surface, a large central pyrenoid penetrated by cytoplasmic channels and radiating into chloroplast lobes, and the presence of a peduncle-homologous microtubular strand. *Palatinus* cells exit the theca through the antapical-postcingular area.

**Key index words:** *Dinophyceae*; *Glenodinium apiculatum*; LSU rDNA; *Palatinus apiculatus*; *Peridinium palatinum*; phylogeny; ultrastructure

**Abbreviations:** ab, accumulation body; b, bacteria; Ch, chloroplast; D, dictyosome; E, eyespot; gv, granule vesicles; LB, longitudinal basal body; LC, layered connective; LF, longitudinal flagellum; LFC, longitudinal flagellar canal; LMR, longitudinal microtubular root; LSC, longitudinal striated collar; LSP, longitudinal sac pusule; N, nucleus; nu, nucleolus; O, oil; P, pyrenoid; pt, pusular tube; s, starch; SBc, striated basal body connective; T, trichocyst; TB, transverse basal body; TF, transverse flagellum; TFC, transverse flagellar canal; TMR, transverse microtubular root; TMRE, transverse microtubular root extension; TSC, transverse striated collar; TSP, transverse sac pusule; TSR, transverse striated root; TSRM, transverse striated root microtubule

As currently defined, the genus *Peridinium* Ehrenb. includes thecate dinoflagellates mostly found in freshwater ponds and swamps. *Peridinium* species share a hypotheca with two similar-sized antapical plates and five postcingular plates and are artificially separated from species of *Peridiniopsis* Lemmerm. by the presence of two to three, rather than zero to one, intercalary plates in the epitheca. Classification of species within *Peridinium* in most 20th-century freshwater dinoflagellate floras incorporates two subdivision levels; the first is the establishment of two groups based on the presence or absence of an apical pore, originally proposed as sections *Poroperidinium* and *Cleistoperidinium* by Lemmermann (1910) and later raised to subgenera by Lefèvre (1932). Each of these subdivisions of the genus is then divided into sets of species, which in general correspond to (or are derived from) the “groupes” originally established by Lefèvre (1932). Species in each group have similar epithelial

<sup>1</sup>Received 8 October 2008. Accepted 20 May 2009.

<sup>2</sup>Author for correspondence: e-mail acalado@ua.pt.

arrangements in terms of number, symmetry, and contacts between plates (Lefèvre 1932, Huber-Pestalozzi 1950, Bourrelly 1970, Starmach 1974). Although generally not regarded as formal taxa (Popovský and Pfister's 1990 use of the term section to designate them is unwarranted), the groups are practical in narrowing down the possibilities when identifying species. However, associations based only on epithelial features do not always result in monophyletic assemblages. This is illustrated by the epithelial tabulation scheme of *Glochidinium penardiiforme* (Er. Lindem.) Boltovskoy, which closely matches that of *Peridiniopsis borgei*, suggesting that the two species belong to the same group (Lefèvre 1932, Huber-Pestalozzi 1950, Popovský and Pfister 1990); in contrast, the presence of three cingular plates in *G. penardiiforme* and six cingular plates in *P. borgei* sets the two species quite apart (Bourrelly 1968, Imamura and Fukuyo 1990, Boltovskoy 1999).

Comparison of species currently included in *Peridinium* with species in related genera (e.g., *Peridiniopsis*, *Glochidinium*, *Protoperidinium* Bergh, *Scrippsiella* Balech ex A.R. Loeb.) suggests the need for revision of the peridinioid group of dinoflagellates. Reconsideration of the phylogenetic affinities of the peridinioids should preferably be based on a combination of complete thecal composition, internal cell structure, and molecular methods. The present article addresses the species included in *Peridinium* group *palatinum* (Lefèvre 1932, Huber-Pestalozzi 1950, Kiselev 1954, Starmach 1974, Popovský and Pfister 1990). Lefèvre named the group after the most common of the included species, for which he used the name *P. palatinum*, although he cited as synonym *P. apiculatum* (Ehrenb.) Er. Lindemann (Lefèvre 1932, p. 102). It is perhaps a consequence of Lefèvre's (1932) magisterial monograph that later authors used Lauterborn's name for the species while acknowledging the synonyms proposed by Lindemann (1928), despite the priority of the epithet *apiculatum* over *palatinum*. The taxonomic and nomenclatural issues surrounding these names are explained in the Discussion.

Although the fine structure of peridinioid cells, in particular the character-rich flagellar base area, is known from few species only, these include the type species of *Peridinium* and *Peridiniopsis* (Calado et al. 1999, Calado and Moestrup 2002). In addition, the database of partial LSU rDNA from dinoflagellates has grown to include numerous comparison points from which phylogenetic hypotheses may be derived (Calado et al. 2006, Moestrup et al. 2006, 2008, Hansen et al. 2007).

#### MATERIALS AND METHODS

*Palatinus apiculatus* occurs commonly in Danish lakes, mostly between October and April. In Portugal, the species was only found in significant numbers in a pond near Vista Alegre, Aveiro, in February 2005. Most of the observations documented herein are from a large population collected from the ponds

Kollelev Mose and Kollelev Hul, north of Copenhagen, in October 1994, and from two cultured strains: AJC1, started from the Kollelev Mose sample and grown in L16 medium (Lindström 1991) supplemented with vitamins according to Popovský and Pfister (1990); and K-34, from the Scandinavian Culture Centre for Algae and Protozoa, started in March 1990 from a freshwater lake in North Sealand, Denmark, initially grown in soil-water medium and later transferred to L16. Cultures were maintained at 14°C, 16:8 light:dark (L:D) photoperiod and a photon flux density of  $\sim 20 \mu\text{mol} \cdot \text{m}^{-2} \cdot \text{s}^{-1}$ .

*Palatinus apiculatus* var. *laevis* was obtained from the Microbial Culture Collection at National Institute for Environmental Studies, Japan, as strain NIES-1405, originally identified as *Peridinium pseudolaevae*.

*Palatinus pseudolaevae* was collected from a pond near Store Magleby, Amager, Denmark, in April 1995, and isolated into culture (strain AJC6) as indicated above for AJC1. Growth in the culture was always moderate, and the strain was eventually lost in 1999.

**LM.** Light micrographs were taken using a Zeiss Axioplan 2 imaging light microscope (Carl Zeiss, Oberkochen, Germany) equipped with a DP70 Olympus camera (Olympus Corp., Tokyo, Japan).

Semi-thin sections (500 nm) for LM were cut with glass knives from the resin blocks used for TEM. Sections were dried on a coverslip, stained with 1% toluidine blue, and mounted in Entellan<sup>®</sup> (Merck KGaA, Darmstadt, Germany).

**SEM.** Both field material preserved in 2% glutaraldehyde and cultured material fixed with Lugol's solution overnight were prepared for SEM. Cells were collected onto Isopore polycarbonate membrane filters with 5 or 8  $\mu\text{m}$  pore size (Millipore Corp., Billerica, MA, USA), rinsed with distilled water, dehydrated through a graded ethanol series, and critical-point-dried. The dry filters were attached onto stubs with double-sided adhesive tape, sputter-coated with gold-palladium or platinum-palladium, and examined using JEOL JSM-6335F (JEOL Ltd., Tokyo, Japan) and Hitachi S-4100 (Hitachi High-Technologies Corp., Tokyo, Japan) scanning electron microscopes.

**TEM.** Two fixation schedules were used: (1) Cells from the 1994 Kollelev Hul sample were transferred with a micropipette into 2% glutaraldehyde in 0.1 M sodium cacodylate, pH 7.4, for 1 h. Following centrifugation (Sigma 302 K centrifuge; Sigma, Osterode/Harz, Germany) and a wash in buffer, cells were postfixed overnight in 0.5% osmium tetroxide prepared in the same buffer. The material was dehydrated through a graded ethanol series and propylene oxide and embedded in Spurr's resin. (2) Swimming cells of *P. apiculatus* from culture K-34 were picked up and transferred to a mixture of 1% glutaraldehyde and 0.5% osmium tetroxide (final concentrations) in 0.1 M phosphate buffer, pH 7.2, for  $\sim 30$  min. After one rinse in buffer, cells were embedded in 1.5% agar and postfixed in 0.5% osmium tetroxide overnight. The agar blocks were dehydrated through a graded ethanol series and propylene oxide and embedded in Epon. Serial sections were prepared using a diamond knife on Reichert Ultracut E and EM UC6 ultramicrotomes (Leica Microsystems, Wetzlar, Germany). Ribbons of sections were picked up with slot grids, placed on Formvar film, and stained with uranyl acetate and lead citrate. Serial sections of four cells were examined using a JEOL JEM 1010 transmission electron microscope.

**Determination of the LSU rDNA sequences from *Palatinus* species.** Partial LSU rDNA sequences for *P. apiculatus* and *P. pseudolaevae* were obtained as described in Daughbjerg et al. (2000).

**DNA of *Peridiniopsis borgei*.** Extracted (total genomic) DNA of a clonal culture (PBSK-1) of the type species of *Peridiniopsis* (viz. *P. borgei*) was kindly provided by Ramiro

Logares. The culture was originally isolated in 2005 by Karin Rengefors from a water sample collected in Stora Kalkbrottsdammen near Malmö, SW Sweden.

**Determination of the LSU rDNA sequence from *P. borgei*.** PCR amplification and temperature cycle conditions were as outlined in Moestrup et al. (2008). PCR fragments were purified using a NucleoFast 96 PCR Kit (Macherey-Nagel GmbH & Co. KG, Düren, Germany) following the recommendations of the manufacturer. A final concentration of 500 ng of the PCR product was air-dried and together with primers sent to the sequencing service at Macrogen (Seoul, Korea) for determination in both directions. The sequencing primers used were D1R, D2C, D3A, D3B, and 28-1483R (for primer sequences, see Daugbjerg et al. 2000 and Hansen et al. 2000).

**Sequence alignment.** The *P. borgei* sequence was added to a data matrix comprising 35 nuclear-encoded LSU rDNA sequences from a diverse assemblage of dinoflagellates retrieved from GenBank (see Table S1 in the supplementary material). Except for the five pfiesteriaceans, the retrieved sequences have previously been determined by our group and used in a number of separate studies (e.g., Daugbjerg et al. 2000, Hansen and Daugbjerg 2004, Bergholtz et al. 2006, Moestrup et al. 2008). The LSU rDNA sequences were aligned using information from the secondary structure with domains and interdomains forming stems and loops as suggested by De Rijk et al. (2000). The alignment comprised 1,439 base pairs, but domain D2 was too variable to be aligned unambiguously. Therefore, this fragment was deleted, thus leaving 1,076 positions to be included in the phylogenetic analyses. The sequence data matrix was manually edited using MacClade (ver. 4.08, Maddison and Maddison 2003).

**Outgroup.** Ciliates (viz. *Tetrahymena pyriformis* and *T. thermophila*) were used for outgroup rooting as molecular studies have revealed these protozoans to form a sister group to the dinoflagellates (e.g., van de Peer et al. 1996).

**Phylogenetic analyses.** The aligned sequence data matrix was subjected to two different methods of phylogeny reconstruction, namely, maximum likelihood (ML) and Bayesian analysis (BA). We used MrModeltest (Nylander 2004) to select the best model among 24 defined models of nucleotide substitution. Following hierarchical likelihood ratio tests, the best-fit model was GTR+I+G, and the value and shape parameter for the proportion of invariable sites ( $\text{pinvar} = 0.2889$ ) and the gamma distribution ( $\text{shape} = 0.5785$ ), respectively, were used in both ML and BA. We used the online version of PhyML (Guindon and Gascuel 2003) available from the Montpellier bioinformatics platform at <http://www.atgc-montpellier.fr/phyml/>. One hundred replicates for bootstrap analyses were run, and a 50% majority-rule consensus tree was calculated using consensus from the Phylip package ver. 3.68 (Felsenstein 2008). This provided bootstrap support values for the branching pattern (Fig. 14). BA was performed using MrBayes (ver. 3.1.2, Ronquist and Huelsenbeck 2003) with a general-time-reversible (GTR) substitution model with base frequencies and substitution rate matrix estimated from the data. In total, 2 million Markov Chain Monte Carlo (MCMC) generations with four parallel chains (three heated and one cold) were performed. A tree was sampled every 50th generation. According to AWTY (Wilgenbusch et al. 2004), the Bayesian analysis had been running long enough as the plots of posterior probabilities of all splits for paired MCMC runs converged using the compare command (plot not shown). Plotting the log-likelihood values as a function of generations in a spreadsheet, the lnL values reached a stationarity level at  $\sim -9.035$  after 10,050 generations. Trees below this level were omitted, and the burn-in thus comprised 39,800 trees. These were imported into PAUP\* (ver. 4b10, Swofford 2003), and a 50% majority-rule consensus

tree was constructed (tree not shown). Posterior probabilities were mapped onto the bootstrap tree derived from the PhyML analysis.

## RESULTS

The organisms examined in this work displayed important differences from typical *Peridinium* species, involving both the theca and the internal organization of the cells. They cannot be accommodated in any existing genus of peridinioid dinoflagellates and are therefore classified in the following new genus.

***Palatinus* Craveiro, Calado, Daugbjerg et Moestrup gen. nov.**

Dinoflagellata autotrophica, thecata, non parasitica. Formula kofoidiana thecarum 4', 2a, 7'', 6c, 5s, 5''', 2''', porus apicalis carens. Patellae laeves vel subtiliter ad grosse granulatae, sed haud areolatae. Lobi chloroplasti ex pyrenoide centrali radians. Pyrenoides canalibus cytoplasmaticis penetratus. Stigma in lobo chloroplasto subter sulcum sito. Filum microtubulare pedunculare praesens sed vesiculae concomitantes carens et tenuis superficie cellulae non accedens (pedunculum non extendans). Cellulae ex theca liberatis per hypovalvam prope antapicem.

**Type species:** *Palatinus apiculatus* (Ehrenb.) Craveiro, Calado, Daugbjerg et Moestrup comb. nov., hic designatus.

Thecate, autotrophic, free-living dinoflagellates. Kofoidian plate formula: 4', 2a, 7'', 6c, 5s, 5''', 2''', apical pore complex absent. Plate surface smooth or finely to coarsely granulate, but not with ridges that form areolae. Chloroplast lobes radiating from a central, branching pyrenoid penetrated by cytoplasmic channels. Eyespot located in a chloroplast lobe beneath the sulcus. Microtubular strand homologous to peduncle microtubules of other dinoflagellates present, but lacking accompanying vesicles and not reaching the cell surface (not extending into a peduncle). Dividing or ecdysing cells exiting the theca through the antapical-postcingular area.

**Type species:** *Palatinus apiculatus* (Ehrenb.) Craveiro, Calado, Daugbjerg et Moestrup comb. nov., designated here.

**Etymology:** The generic name is derived from the specific epithet of *Peridinium palatinum*, so named in allusion to the Palatinate (Pfalz, in German), the southwest region of Germany where Lauterborn (1896) originally found the species. As the name of a genus, the term is treated as a noun and takes the masculine gender (Lewis and Short 1879).

**Note:** The choice of the generic name *Palatinus* aims to preserve the link to the specific epithet long used for the type species, while replacing it with its long-accepted older synonym (see Discussion). Conservation of the specific epithet *palatinum* does not seem desirable as the generic name is being changed. The original publication by

Ehrenberg (1838) of illustrations where the species can be recognized, against the absence of illustrations accompanying Lauterborn's original description of *Peridinium palatinum*, and the recent use of the legitimate name *Peridinium apiculatum* (Ehrenb.) Claparède et J. Lachmann (Hansen and Flaim 2007), also speak for the application of the priority principle in this case.

*Palatinus apiculatus* (Ehrenb.) Craveiro, Calado, Daugbjerg et Moestrup comb. nov. (Fig. 2, a–e).

*Basionym*: *Glenodinium apiculatum* Ehrenberg 1838. *Infusionsthierchen*, p. 258, pl. XXII, fig. XXIV (reproduced here in grayscale as Fig. 1).

*Homotypic synonyms*: *Peridinium apiculatum* (Ehrenb.) Claparède and Lachmann (1859, p. 404); *Properidinium apiculatum* (Ehrenb.) Meunier (1919, p. 60); “*Peridinium apiculatum* (Ehrenb.) Er. Lindemann” (1928, p. 260), later isonym.

*Heterotypic synonyms*: *Peridinium palatinum* Lauterborn (1896, p. 17); *Peridinium marssonii* Lemmermann (1900a, p. 28); *Peridinium anglicum* G. S. West (1909, pp. 187–90, fig. 23).

*Palatinus apiculatus* var. *laevis* (Huitfeldt-Kaas) Craveiro, Calado, Daugbjerg et Moestrup comb. nov. (Fig. 13, a–c).

*Basionym*: *Peridinium laeve* Huitfeldt-Kaas 1900. *Vid.-Selsk. Skr. [Christiania], Math.-Naturv. Kl. 1900* No. 2:4, figs. 1–5.

*Homotypic synonyms*: *Peridinium palatinum* f. *laeve* (Huitfeldt-Kaas) Er. Lindemann (1925a, p. 478); *Peridinium apiculatum* f. *laeve* (Huitfeldt-Kaas) Er. Lindemann (1928, p. 260); “*Peridinium palatinum* f. *laeve* (Huitfeldt-Kaas) M. Lefèvre” (1932, p. 105), later isonym.

*Note*: This taxon has often been ranked as a *forma* by the modern authors that recognize it. However, we doubt the usefulness of having two infraspecific categories for unicellular organisms, particularly when choice of rank has been irregular and inconsistent (see established varieties and forms of freshwater dinoflagellates in, e.g., Starmach 1974). We therefore use the higher-ranking *varietas*.

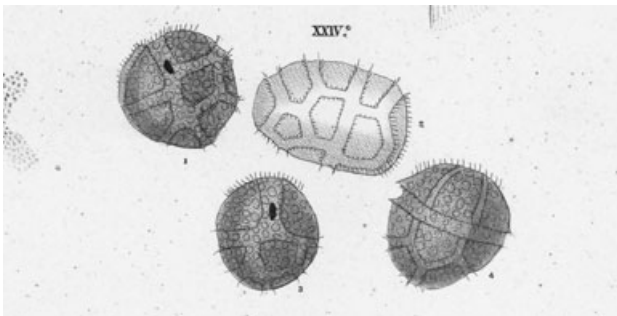


FIG. 1. *Glenodinium apiculatum*. Reproduced from Ehrenberg (1838, pl. XXII, fig. XXIV). Same size as the original drawing.

*Palatinus pseudolaevus* (M. Lefèvre) Craveiro, Calado, Daugbjerg et Moestrup comb. nov. (Fig. 13, d–i).

*Basionym*: *Peridinium pseudolaeve* M. Lefèvre 1926. *Rev. Algol.* 2:341, pl. XI, figs. 6–9, ‘*pseudo-laeve*’.

*Note*: Lefèvre (1926, pp. 338–41) noted that *P. pseudolaeve* had been illustrated under the name *P. laeve* by Lindemann (1920, p. 128, fig. 18). However, he later (Lefèvre 1932, p. 108) cited in error Lindemann (1919), which does not contain any illustration showing *P. pseudolaeve* characters. The erroneous citation has been repeatedly copied (Schiller 1937, Starmach 1974, Popovský and Pfister 1990).

*Observations of Palatinus apiculatus. Morphology and thecal structure*: Cell size was mostly in the range of 32–48  $\mu\text{m}$  long, 28–42  $\mu\text{m}$  wide, and 23–28  $\mu\text{m}$  thick, with the largest values measured in heavily ornamented field specimens with sutures up to 3  $\mu\text{m}$  wide. The cells were ovoid, with the hypotheca more rounded than the tapering, somewhat conical epitheca, and were nearly flat on the ventral side (Fig. 2, a–e). In ventral view the epitheca showed a characteristic twist to the left relative to the hypotheca, leaving plate 7'' vertically aligned with the right sulcal plate and plate 1' in line with the right side of plate 1''' (Fig. 2, a and c). The four apical and the two intercalary plates usually showed a markedly asymmetric arrangement, centered around an elongate 3', oriented from dorsal-left to ventral-right and pointed on the ventral side (Fig. 2d). Intercalary plate 2a was the longest, oriented roughly parallel to 3' and contacting plates 4'', 5'', and 6'' (Fig. 2d). In well-ornamented cells, the edges of the five uppermost plates (2', 3', 4', 1a, 2a) were raised to form smooth flanges up to 2  $\mu\text{m}$  high (Fig. 2, a, b, and d); the edges of the remaining epithelial plates were less raised and were provided with granules or short, blunt spines (Fig. 2, a, b, and d).

The cingulum was a distinct groove that circled the cell transversely, descending about its own width at the distal (right-ventral) end. The first two cingular plates were short, both essentially positioned above plate 1''' (Fig. 2a). Plates c3–c6 were roughly aligned with plates 2'''–5''', respectively (Fig. 2, a and e). Dissection of the sulcus revealed four larger plates (Fig. 2, a and c, only three sulcal plates indicated) and a smaller one intercalated between the right and left sulcal plates and the posterior plate; both this small so-called accessory plate and the left sulcal plate were usually concealed in intact thecae of *P. apiculatus* and were easier to see in specimens of *P. apiculatus* var. *laevis* and *P. pseudolaevus* (see below).

The sulcus was bordered by the raised edges of plates 1''' and 5''' (Fig. 2, a and c). The edges of postcingular and antapical plates were provided with conical spines, which reached up to 2.5  $\mu\text{m}$  long in the antapical area of heavily ornamented cells

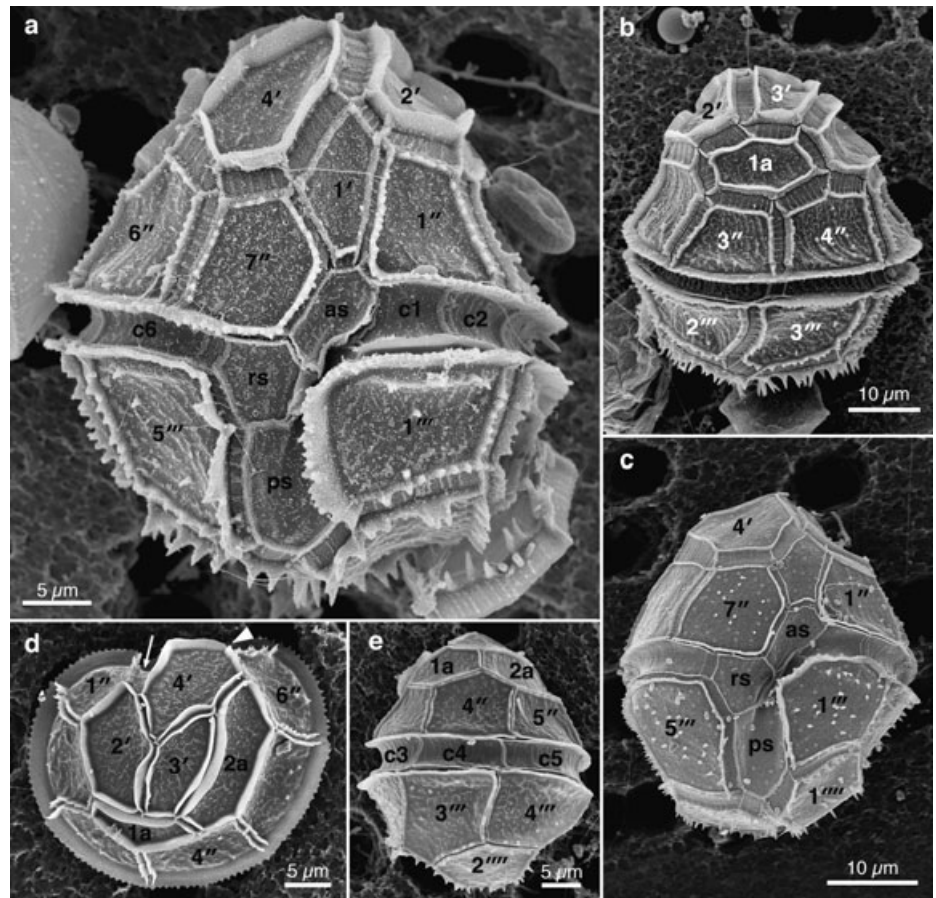


FIG. 2. *Palatinus apiculatus*, SEM. All cells from field samples except cell in (c), which is from strain K-34. as, anterior, rs, right, and ps, posterior sulcal plates. (a) Ventral view of a strongly ornamented cell; note the shorter cingular plates c1 and c2 positioned for the most part above plate 1'''. (b) Dorsal view. (c) Ventral view. (d) Apical view showing the asymmetric arrangement of the apical and intercalary plates. The thin arrow indicates the plate 1', and the arrowhead indicates the position of plate 7''. (e) Dorsal view of small cell with narrow sutures between the plates.

(Fig. 2a). Shorter and blunter spines were scattered along the surface of some plates, especially in the hypotheca (Fig. 2, a–e).

Elongated groups of tiny granules usually gave a rough appearance to the plate surface of field-collected specimens (Figs. 2, a and b; 3a), whereas cells from cultures looked smoother (Fig. 2c). Numerous pores with raised rims were distributed on the surface of all plates, especially near their margins; the outer pore opening was ~200–250 nm in diameter and was sometimes associated with a trichocyst (Fig. 3b). When viewed in SEM, most pores contained a round structure in the middle (Fig. 3a, arrow); in TEM, this probably corresponded to a cylindrical, hollow structure, located between the plasma membrane and the amphiesmal vesicle, and associated with a granular, subthecal vesicle (Fig. 3c).

The sutures between plates varied from thin lines in small specimens (Fig. 2e) to bands up to 2.5–3 μm wide in large cells (Figs. 2, a–c; 3a). Cross-striations in the sutures were visible, but not striking, in high resolution LM (not shown). In SEM, the striations were lines 0.15–0.2 μm wide placed some 0.8–0.9 μm apart (Fig. 3a).

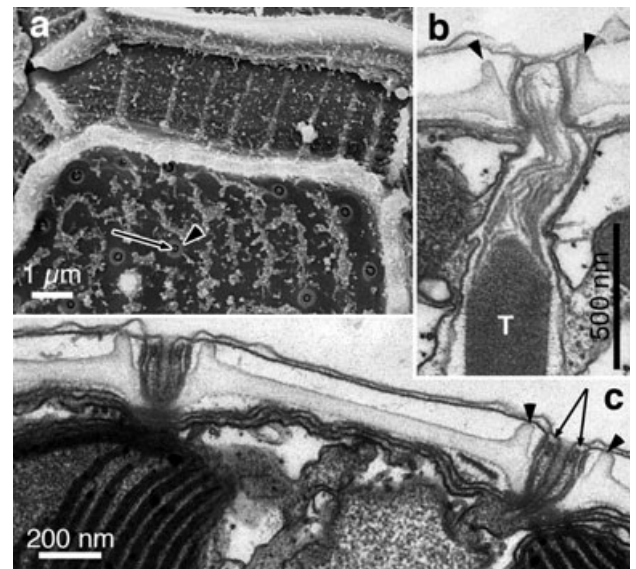


FIG. 3. *Palatinus apiculatus*, thecal structure. (a) Plate surface showing pores (arrowhead points to pore rim) containing round structures (arrow). Note the thin striations on the suture. SEM. (b) Section through a pore connected to a trichocyst (T). Arrowheads point to pore rim. TEM. (c) Pores connected to cylindrical hollow structure (arrows). TEM.

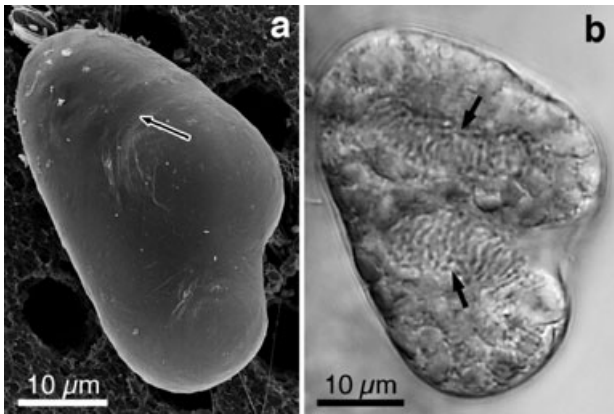


FIG. 4. *Palatinus apiculatus*. Division in a naked, motile stage. (a) Ventral view, SEM. The arrow indicates the left part of the cingulum. (b) Light micrograph showing the two recently separated nuclei (arrows). Lightly stained with acetocarmine.

Dividing or recently divided cells exited the theca through the antapex, leaving the empty thecae with missing or displaced antapical and sometimes also postcingular plates (not shown). Although division stages were rarely seen in the cultures, unarmored, swimming dividing cells were abundant in the dense populations collected from Kollelev. Figure 4 shows the typical appearance of these naked division stages, with the posterior ends of the forming cells diverging in an asymmetrical way; the shallow left side of the cingulum was barely visible in SEM (Fig. 4a, arrow), and two recently divided nuclei were readily evidenced by lightly staining with acetocarmine (Fig. 4b).

**General structure in LM and TEM:** The cell surface was nearly covered with brownish chloroplast lobes, which radiated from a central pyrenoid (Figs. 5, a and b; 6, a and b). The nucleus was transversely elongated and occupied the dorsal part of the cell at cingulum level, slightly invading the epicone (Figs. 5, a and b; 6, a and c). Swimming cells usually contained a large vesicle on the ventral-right side, here called a longitudinal sac pusule (LSP; see below) (Figs. 5a; 6, c and d); this was often lacking in immotile specimens. Oil droplets were found in the peripheral part of the cell, mostly in the epicone, whereas starch grains accumulated mainly in the hypocone (Fig. 6a). Bacteria were plentiful in the cytoplasm of cultured cells, especially near the central pyrenoid, between the radiating chloroplast lobes (Figs. 6, a–c; 7a), and in the ventral region (Fig. 8a). Bacteria were also found inside the nucleus of some cells (Figs. S1, b and c, in the supplementary material). In all cases, bacteria were bounded by two membranes and surrounded by an electron-translucent area ~20–80 nm thick, with no external membranes separating them from either the cytoplasm or the nucleoplasm of the dinoflagellate (Figs. S1c; 8c). Dictyosomes were scattered around the central pyrenoid (Fig. 7a) and near the

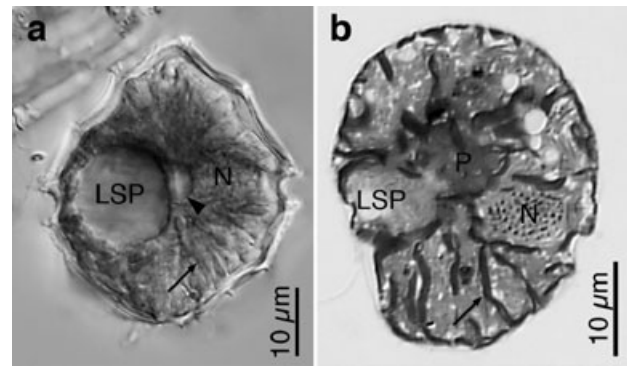


FIG. 5. *Palatinus apiculatus*, general view in LM. Thin arrows indicate chloroplast lobes radiating from the center. N, nucleus; LSP, longitudinal sac pusule. (a) Ventral view of a whole, fixed cell. The arrowhead points to the extended transverse flagellar canal (transverse sac pusule). (b) Semithin section through the longitudinal axis, viewed from the cell's left. P, central pyrenoid.

nucleus (Fig. S1c). Trichocysts were common in the peripheral cytoplasm (Figs. 6a; 7a). Accumulation bodies with unrecognizable contents were present in the epicone (Fig. 6, a, c). Two types of vesicles were common along the surface, apparently discharging their contents into amphiesmal vesicles: round vesicles containing what seemed to be whorls of membranous material (Fig. 7d), and ellipsoid vesicles with a granular matrix and several lumps of electron-opaque material (Fig. 7, a, d). Vesicles with fibrillar contents of the type usually associated with flagellar hairs were seen in close association with dictyosomes; Figure S1a documents traffic of small vesicles between a dictyosome and a fibrillar vesicle. Vesicles containing crystal-like bodies were common throughout the cytoplasm (Fig. 8a), including the ventral area near the basal bodies (Fig. S2, b and d, in the supplementary material).

**Chloroplast, pyrenoid, and eyespot:** Chloroplast lobes radiated from the central pyrenoid in all directions and ramified into further lobes, establishing what was probably a single chloroplast network (Figs. 5b; 6, a–c; 7a). Upon reaching the peripheral cytoplasm, the lobes extended tangentially, covering most of the surface (Figs. 5b; 6a). Sections through the center of the cell showed the three-thylakoid lamellae regularly arranged in evenly spaced, parallel alignments (Fig. 7a). In some chloroplast lobes, the peripheral lamella surrounded the internal lamellae in a way reminiscent of the girdle lamellae of heterokonts (Fig. 7b). The central pyrenoid extended somewhat into the radiating lobes, giving a fragmented appearance in sections through its periphery (Fig. 6b). The pyrenoid matrix contained a few scattered thylakoid lamellae and was traversed by cytoplasmic channels of irregular shape (Figs. 6, a, b; 7a); Fig. 7c shows two such cytoplasmic channels lined by the three membranes of the chloroplast envelope. Thylakoid-free areas were also present in some peripheral chloroplast lobes (Fig. 7a).

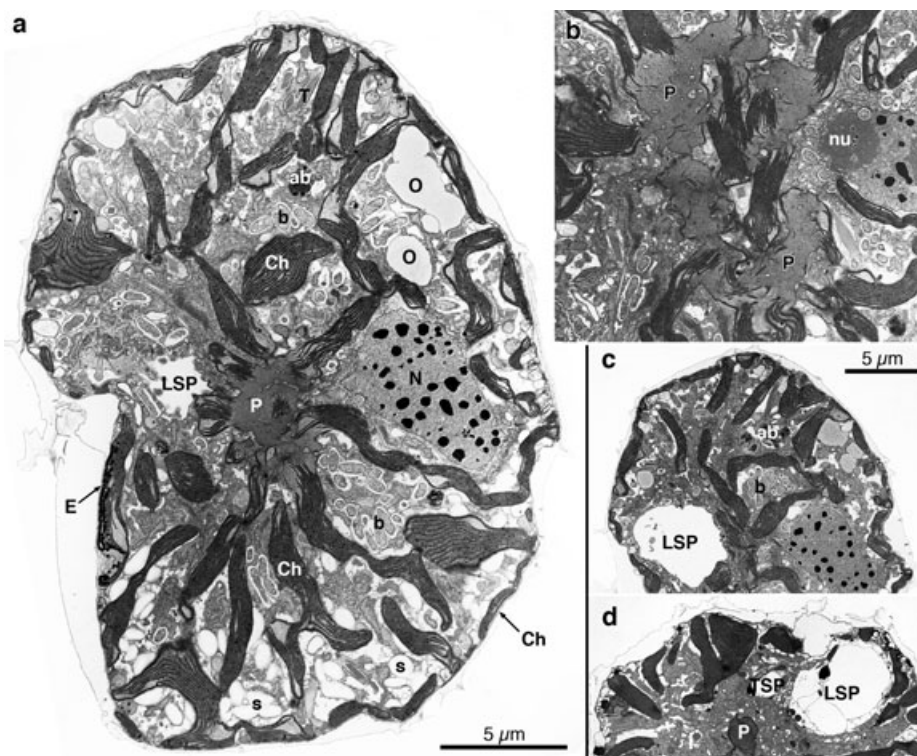


FIG. 6. *Palatinus apiculatus*, general ultrastructure, TEM. (a) Longitudinal section viewed from the cell's left showing the central pyrenoid (P) and the radiating chloroplast lobes (Ch), groups of bacteria (b), the nucleus (N), the eyespot (E) in the ventral region, and the left side of the longitudinal sac pusule (LSP); oil droplets (O) are visible in the epicone and starch grains (s) in the hypocone. (b) Detail of the central pyrenoid (P) sectioned through its peripheral, branching part, showing scattered thylakoid lamellae and cytoplasmic tubes. Scale bar as in (a). (c) Longitudinal section of the same cell as in (a), but farther to the right side, showing the LSP occupying most of the midventral area. (d) Approximately transverse section viewed from the anterior-right side of the cell, showing the LSP and the much smaller (but not collapsed) transverse sac pusule (TSP). Cell fixed from field material. Scale bar as in (c). ab, accumulation body; nu, nucleolus.

The eyespot was usually visible with the light microscope, although often faintly, as a reddish area nearly 5  $\mu\text{m}$  long located in the upper part of the sulcus. It consisted mainly of one to two layers of globules along the ventral surface of a chloroplast lobe, placed directly underneath the chloroplast envelope (Fig. 8, a and b). Although layers of globules oriented parallel to the surface were in general not separated by thylakoids, some layers turned obliquely inward, alternating with obliquely oriented thylakoid lamellae (Fig. 8, a and b). The size of individual globules ranged from 80 to 130 nm.

**Pusular system:** Typical pusular elements, that is, membrane-bounded compartments wrapped in a vesicle, were of two kinds: roughly cylindroid tubes with the lumen some 150–300 nm in diameter, and flat vesicles with relatively straight profiles up to nearly 4  $\mu\text{m}$  long (Fig. 7a). The tubes opened at the flagellar canals and radiated from the ventral area, with some twists and turns along their path but without ramifications. A single tube connected to the dorsal-posterior side of the longitudinal flagellar canal (LFC) and extended into the posterior-ventral-left part of the cell (Fig. 8a). Two tubes extended from the transverse flagellar canal, one

roughly parallel to the tube originating at the LFC, but deeper into the cell, and the other oriented toward the anterior-ventral area (Fig. S2, a, b and d; see the proximal ends of the tubes in the diagram of Fig. 9). The flat vesicles extended parallel to the three tubes (Fig. 7a) but were absent from the flagellar base area. We could not demonstrate continuity between the flat vesicles and the tubes nor any other structure. Two large vesicles were connected to the flagellar canals and were therefore labeled sac pusules in the sense of earlier light microscopists, as explained by Calado et al. (1999). The largest of these was a round vesicle up to > 10  $\mu\text{m}$  in diameter, located on the ventral-right side of the cell and connected to the LFC (Figs. 5a; 6, c and d; 8a). Whereas the connection between this LSP and the LFC was rather wide in cells initially fixed with glutaraldehyde alone, it was constricted to a narrow bridge when osmium tetroxide was included in the first fixation (Fig. 8a). The transverse flagellar canal (TFC) extended into a much smaller vesicle, which was sometimes visible with the light microscope (Fig. 5b) but was collapsed in cells fixed with the mixture of glutaraldehyde and osmium tetroxide (compare Fig. 6d with Fig. S2, a–f). Although profiles of

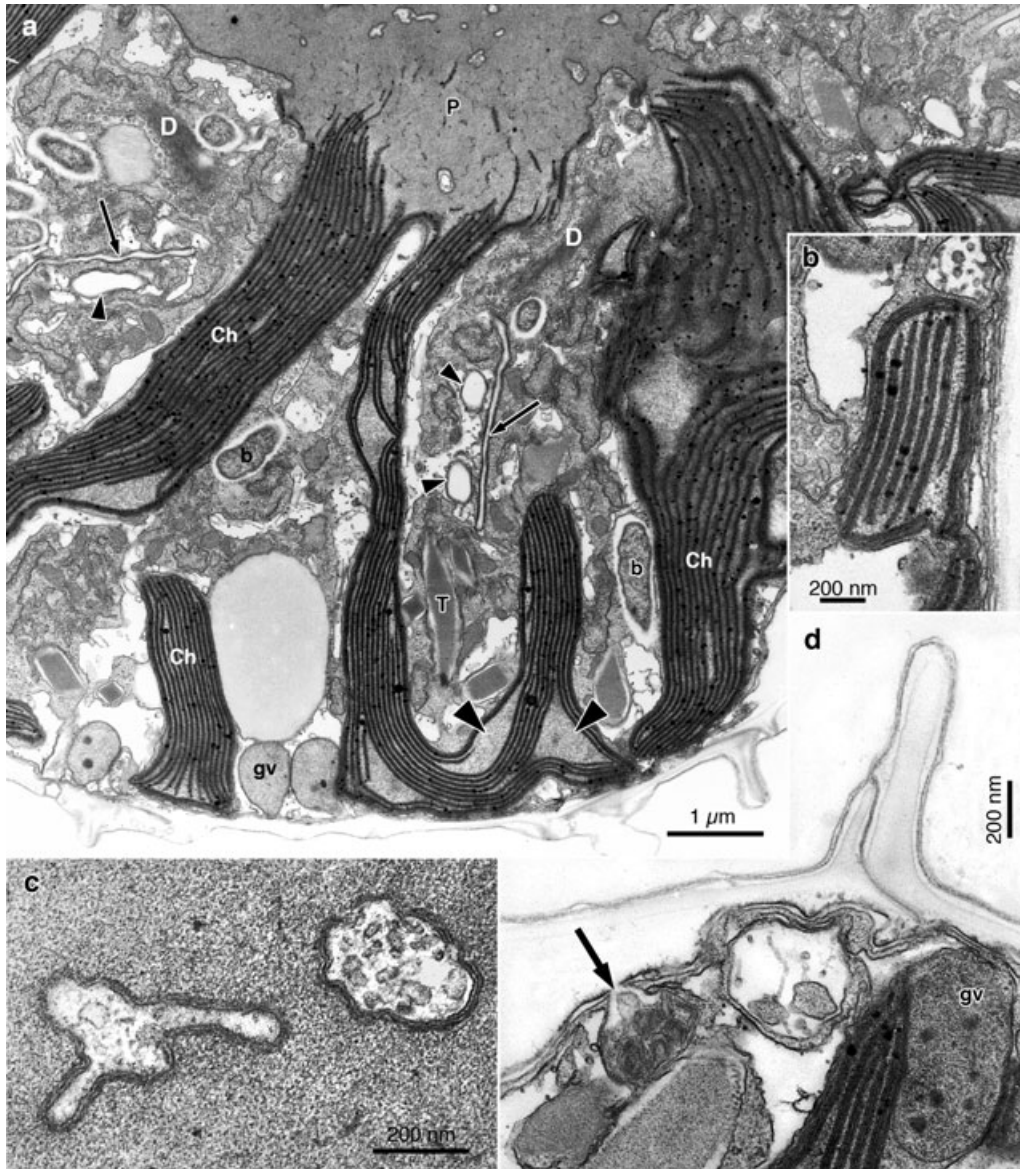


FIG. 7. *Palatinus apiculatus*, general ultrastructure. gv, granular vesicle; T, trichocyst. (a) Longitudinal section showing part of the central pyrenoid (P), chloroplast lobes (Ch) with some areas free of thylakoids (large arrowheads), and dictyosomes (D). Thin arrows point to the flat pusular vesicles, and small arrowheads indicate pusular tubes. (b) Detail of a chloroplast lobe with a peripheral lamella overlapping the ends of internal lamellae. (c) Cytoplasmic tubes in the pyrenoid, bounded by three membranes. (d) Vesicles with membranous contents (the arrow marks a connection with an amphiesmal vesicle) and vesicles with granular contents (gv), both common along the cell surface.

endoplasmic reticulum were common along the surface of the sac pusules, direct connection between the sac pusules and typical pusular elements was not observed.

**Flagellar apparatus:** A diagram of the flagellar apparatus and related structures of *P. apiculatus* as seen from the cell's left is given in Figure 9. The same point of view is illustrated in a series of sections progressing from left to right in Figures S2, 10, and 11. A slightly different view, from an anterior-left perspective, is given in Figure 12. As estimated from serial sections, the basal bodies

formed an angle of about 80°–85°. Each flagellum exited the cytoplasm into an area bounded by a single membrane and connected to the exterior by a pore; complete rings of fibrous material, which appeared striated in some views and were labeled striated collars, surrounded the pores of these so-called flagellar canals. Figures S2f and 12a show fibrous material extending from the transverse striated collar (TSC) that established continuity between the two collars.

A multi-stranded microtubular root extended from the basal body region, along the surface of the

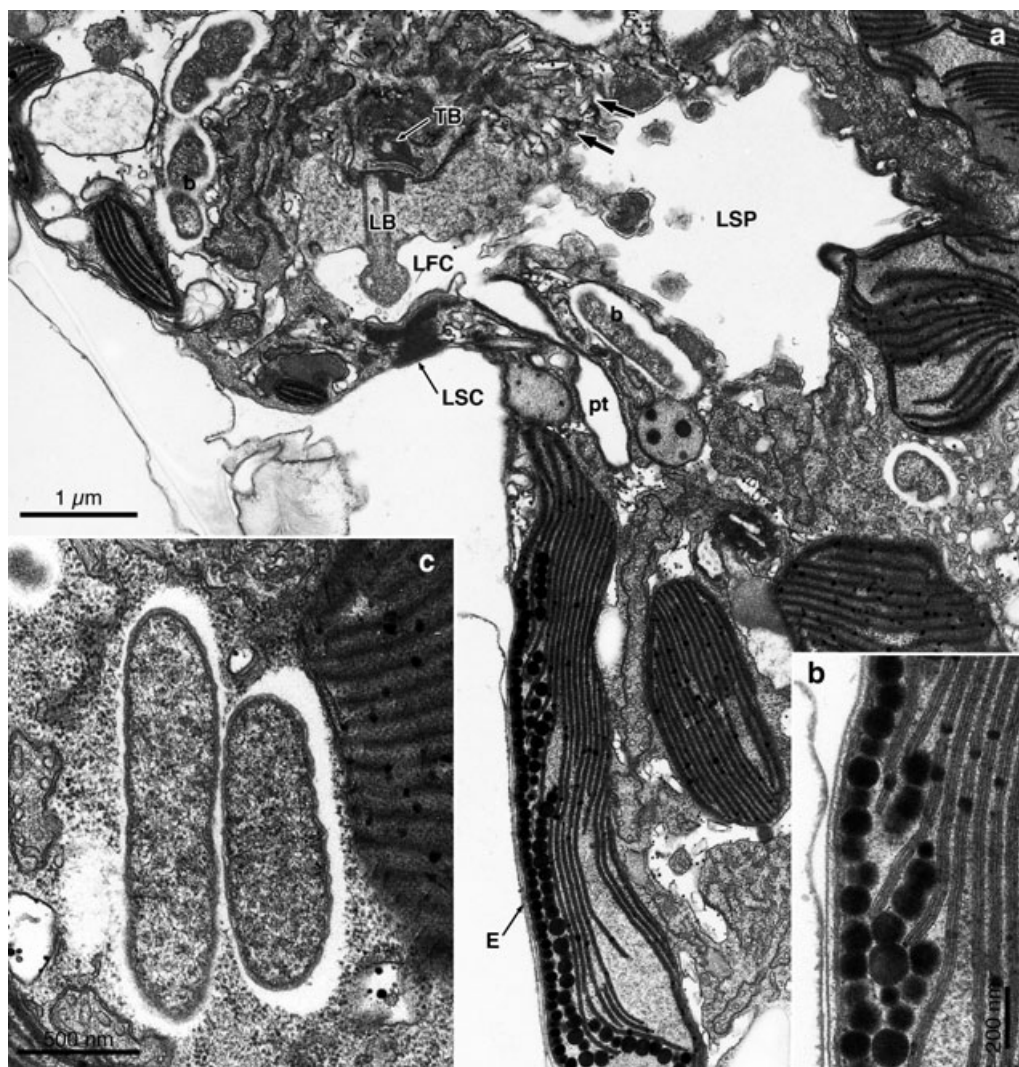


FIG. 8. *Palatinus apiculatus*, ultrastructure of the ventral area. (a) Longitudinal section showing the eyespot (E) and the basal bodies (LB and TB). Note the connection of the longitudinal sac pusule (LSP) and of a pusular tube (pt) to the longitudinal flagellar canal (LFC). LSC, longitudinal striated collar; b, bacteria. The arrows indicate vesicles with crystal-like contents. (b) Layers of globules in the eyespot, the inner layer repeatedly bending inward along obliquely oriented thylakoid lamellae. (c) Bacteria, bounded by two membranes and surrounded by an electron-translucent area.

sulcus, toward the antapex. We refer to it as the longitudinal microtubular root (LMR; designated r1 in Moestrup 2000), and its principal associations are shown in Figure 10. The rightmost microtubule of the LMR associated with the proximal part of the longitudinal basal body (LB) (Fig. 10, g and h). We estimated about five LMR microtubules at this proximal level, and the number increased gradually to an estimated 40 in the sulcal region, overlying the eyespot. The LMR passed along the surface of the longitudinal striated collar (LSC), to which it was probably attached, although a distinct fiber between the two structures was not seen (Fig. 10, d and f). The dorsal side of the proximal part of the LMR was covered with a layer of electron-opaque material (Figs. S2, f and g; 10, a–h), from which three fibers extended toward three or

four triplets of the TB, some 500–600 nm from its base (Fig. 10, c and d). A layered connective (LC) linked this dorsal layer of the LMR with the proximal end of the transverse basal body (TB) (Fig. 10, f–h). A single fiber connected one of the triplets of the proximal part of the TB and the rightmost microtubules of the LMR and continued toward the base of the LB (Fig. 10, g and h). Figure 10, g and h, and 11a show the LC extending to the right beyond the LMR and directly connecting the two basal bodies. In exact cross-sections of the structure (i.e., longitudinal sections of the cell), the LC was ~120 nm thick with two outer electron-opaque layers 30 nm thick and two middle layers, each thinner than a unit membrane, limiting an area with discontinuous electron-opaque material (Fig. 10h). The LC extended for nearly 500 nm along the left-right

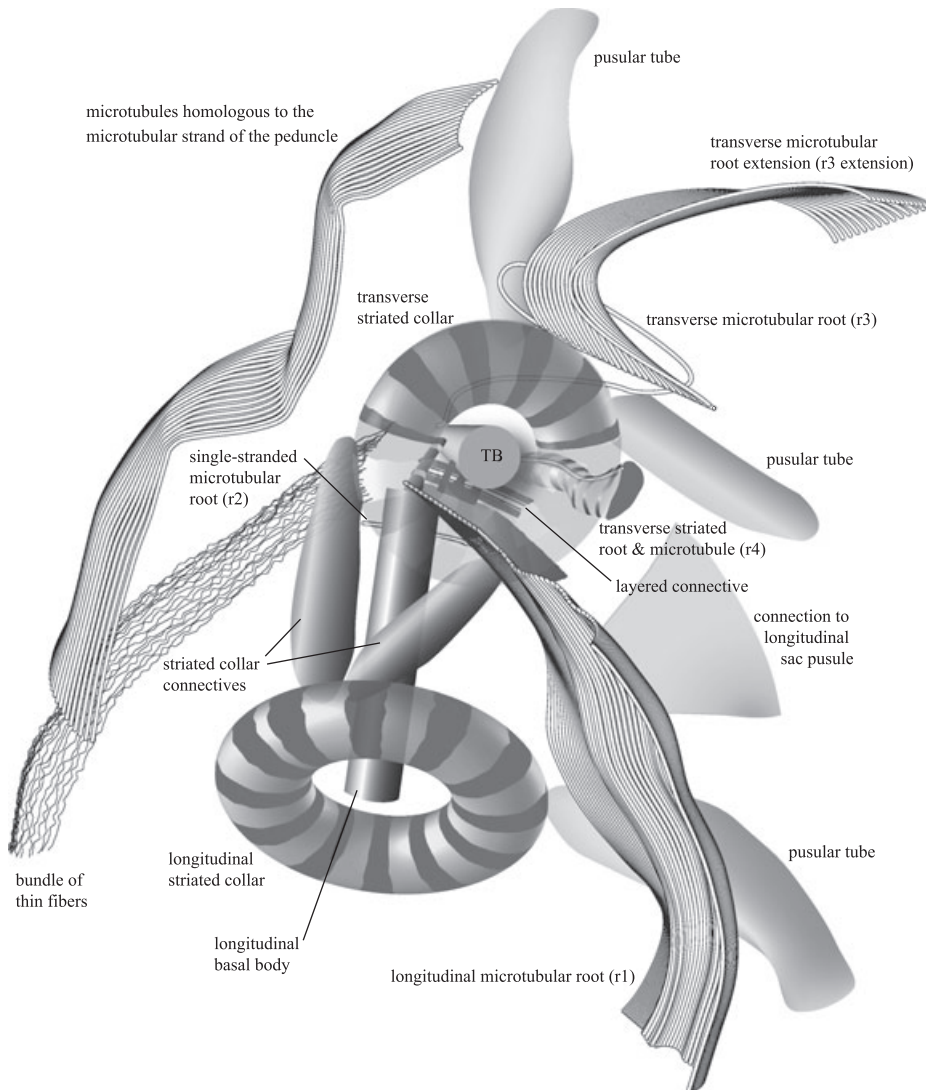


FIG. 9. *Palatinus apiculatus*. Schematic representation of the flagellar apparatus and adjacent structures as viewed from the cell's left (transverse basal body, TB, in cross-section).

axis and slightly less along the ventral-dorsal axis (Figs. 10, f–h; 11, a and b).

A single-stranded microtubular root (SMR; r2 in Moestrup 2000) was oriented parallel to the LMR and extended from the right side of the LB to near the dorsal side of the LSC (Fig. 11, b–d).

A layer of electron-opaque material, apparently continuous with the upper layer of the LC, surrounded the base of the TB, linking the two opposite sides where roots associate with this basal body (Figs. 10, g and h; 11a). On the apical, slightly ventral side of the TB, a single microtubule ran parallel to the triplet microtubules for some 300 nm (Fig. 10, e–h), then turned away and took a sharp turn to the left, passing around the TFC next to a row of collared pits, spiraling anticlockwise for about one and a half turns (Figs. S2, a–g; 10, a–c). This transverse microtubular root (TMR; r3 in Moestrup 2000) nucleated one or two rows of about 20 microtubules, the TMR extension (TMRE), which curved around the anterior part of the TFC

and continued toward the pyrenoid for  $\sim 1.4 \mu\text{m}$  (Fig. S2, a–d).

A fiber associated with the dorsal-posterior side of the TB and with the anterior layer of the LC extended toward the cell's left for  $2.5 \mu\text{m}$  and terminated on the surface, near the left end of the TSC (Figs. S2, a, b, d–g; 10, a–f). This was identified as the transverse striated root (TSR) and was accompanied by a microtubule (TSRM; r4 in Moestrup 2000), which diverged from the fiber near the proximal end and connected with the posterior layer of the LC (Fig. 10, d, e). A conspicuous set of concentric arcs of electron-opaque material, roughly centered on the TB, partly occupied the area anterior to the proximal end of this basal body (Figs. 10, f–h; 11, a–c).

A strand of about 16 microtubules was seen near the flagellar collars and roots without visible connections to these structures. It was present near the TMR and TMRE microtubules (Fig. S2b) and continued toward the posterior-ventral side, bending

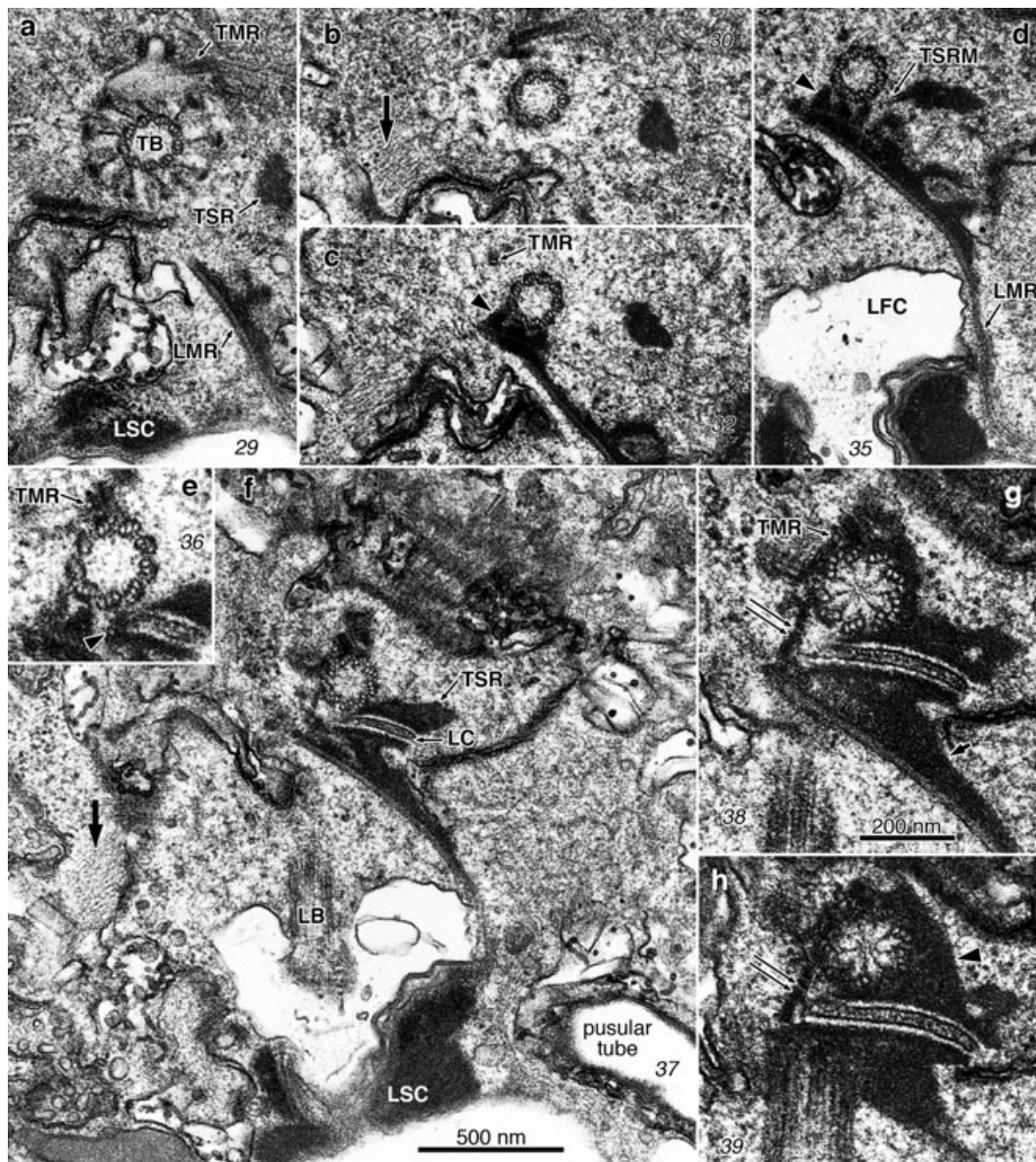


FIG. 10. *Palatinus apiculatus*, flagellar apparatus. Same series as in Figure S2 (in the supplementary material). Small slanted numbers refer to the section number. Proximal part of the transverse microtubular root (TMR), approaching and connecting to the anterior face of the transverse basal body (TB). The thick arrow in (b) and (f) points to a bundle of thin fibers extending along the flagellar base area, on the ventral side. (a–e) The transverse striated root (TSR) approaches the TB from the posterior-dorsal side. The TSR microtubule (TSRM) diverges from the fibrous portion of the root and connects to the posterior layer of the layered connective [LC; arrowhead in (c)]. The triple connection between the TB and electron-opaque material on the dorsal face of the LMR is marked with an arrowhead in (c) and (d). (f–h) A fiber connects the TB with the proximal end of the LMR [double arrow in (g) and (h)], apparently extending to the longitudinal basal body (LB) in (h). Arrowhead in (h), electron-opaque material extending from the LC and surrounding the base of the TB. LMR, longitudinal microtubular root.

near the surface of the TSC and barely reaching the level of the LSC (Figs. S2e; 12, a and b), but it did not extend beyond these areas. An accumulation body was usually adjacent to this row of microtubules (Fig. S2b). A bundle of thin fibers coming from near the TSC seemed to extend beyond the posterior ends of the microtubules toward the posterior-ventral side, ending near the ventral cell surface (Figs. 10, b, c, and f; 12, b and c).

*Morphology and thecal structure of Palatinus apiculatus var. laevis (strain NIES-1405).* Most specimens fell in the length range of 26–30  $\mu\text{m}$  and were somewhat less elongate than the populations examined of *P. apiculatus*. Other than that, their overall characteristics were similar to cultured material of *P. apiculatus*, including the very thinly striated sutures in larger specimens and the presence of distinct spines in the hypotheca (Fig. 13, a–c).

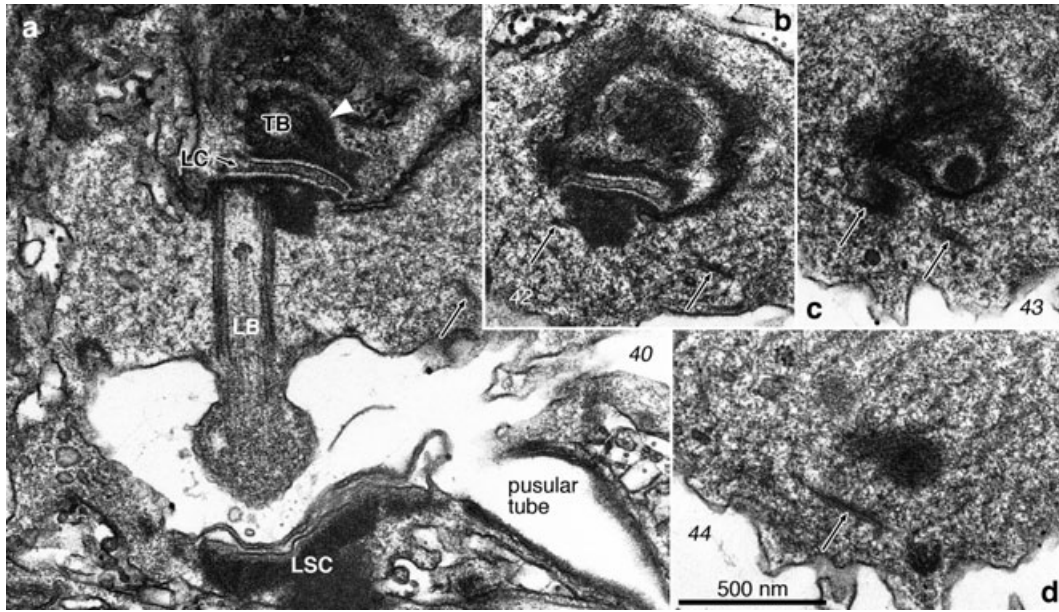


FIG. 11. *Palatinus apiculatus*, flagellar apparatus. Same series as Figure S2 (in the supplementary material) and Figure 10. Small slanted numbers refer to the section number. Single-stranded microtubular root (arrows) associated with the right hand side of the longitudinal basal body (LB). The proximal end of the transverse basal body (TB) is covered by electron-opaque material [arrowhead in (a)] that contacts also the upper layer of the layered connective (LC). LSC, longitudinal striated collar.

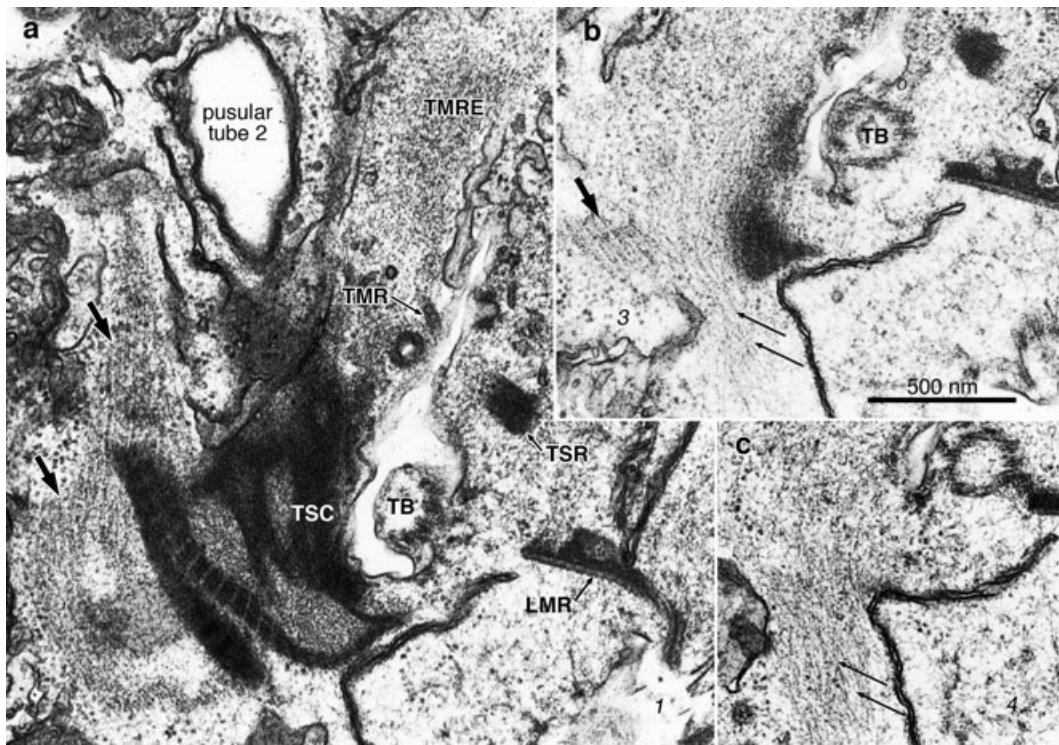


FIG. 12. *Palatinus apiculatus*, flagellar apparatus. Nonadjacent serial sections proceeding from anterior-left to posterior-right, viewed from the left. Strand of microtubules adjacent to the flagellar base area (thick arrows) and a roughly parallel bundle of thin fibers (thin arrows) that extends beyond the posterior end of the microtubules. The microtubular strand runs adjacent to fibrous material extending from the transverse striated collar (TSC). LMR, longitudinal microtubular root; TB, transverse basal body; TMR, transverse microtubular root; TMRE, transverse microtubular root extension; TSR, transverse striated root.

Figure 13b shows slightly raised borders of apical plates similar to those of cultured *P. apiculatus* (compare with Fig. 2c). However, the apical and intercalary plate pattern varied from nearly totally symmetric (Fig. 13c) to slightly asymmetric with plate 3' somewhat elongate in a dorsal-left to ventral-right orientation (Fig. 13b), without reaching the marked asymmetry seen in *P. apiculatus*. The left side of the sulcus was usually less excavated than in *P. apiculatus*, making it easier to document the left and accessory sulcal plates (Fig. 13a).

**Morphology and thecal structure of *Palatinus pseudolaevis*.** Most cells were 28–37  $\mu\text{m}$  long, 25–35  $\mu\text{m}$  wide, and 24–28  $\mu\text{m}$  thick. The cells were ellipsoidal, slightly flattened dorsoventrally, with the epitheca and hypotheca of similar size. The general appearance was usually smoothly convex (Fig. 13d); the concavity of plates seen in Figure 13, e, f, h,

and i, is an artifact produced during electron microscopical observation. The cells displayed the characteristic twist to the left of the epitheca relative to the hypotheca, as described for *P. apiculatus* (Fig. 13d). The tabulation matched that of *P. apiculatus* in terms of number and position of plates, but the apical arrangement of plates was regularly symmetrical (Fig. 13e). The cingulum descended near the right-ventral side about a cingular width (Fig. 13d). Although bordered by the raised edges of plates 1''' and 5''', the sulcus was usually wide enough to allow visibility of all five sulcal plates (Figs. 13, d and g). Scattered granules or short, blunt spines ornamented some of the thecal plates, particularly in the hypotheca (Figs. 13, d and i), but no conical spines were present. Sutures between plates were distinctly striated, with individual cross-lines just over 0.2  $\mu\text{m}$  thick and topped

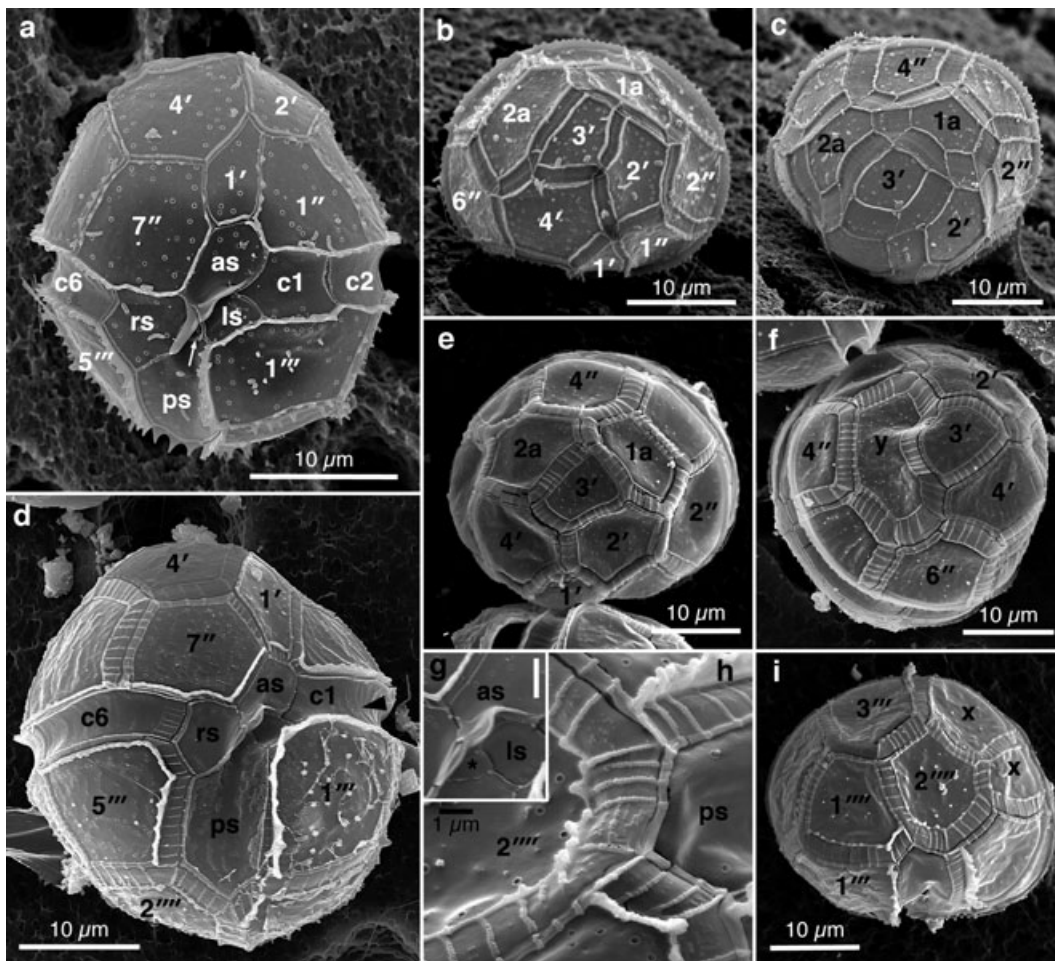


FIG. 13. *Palatinus apiculatus* var. *laevis* (a–c) and *P. pseudolaevis* (d–i), SEM. All cells from cultures. as, anterior; rs, right; ls, left; and ps, posterior sulcal plates. (a) Ventral view. (b, c) Apical views showing large sutures with thin cross-striations. The apical plates show a more symmetric arrangement than in *P. palatinus*. (d) Ventral view. (e) Apical view with the characteristic symmetric arrangement of the four apical and two intercalary plates. (f) Apical view showing plate variation; one transversely elongate plate (y) occupies the position of the two intercalary plates. (g) Detail of the sulcal plates showing the small accessory plate (\*). Scale bar, 2  $\mu\text{m}$ . (h) Detail of plate and suture surfaces. (i) Antapical view. Plate variation; plate 4''' (or perhaps 3''') appears subdivided (plates marked with x).

by a row of small granules (Fig. 13h). The cells exited the theca through the antapex (not shown).

Cells with variant tabulations were relatively common in the culture. Variations most commonly affected epithelial plates, particularly the fusion of the two intercalary plates (Fig. 13f, plate marked y). Figure 13i shows a more uncommon variation, in which there are six postcingular plates, apparently caused by the duplication of plate 4''' (or perhaps 3''').

**Molecular phylogeny.** The tree topology obtained from ML using PhyML is illustrated in Figure 14. The deepest branches in the tree are very short and without support from bootstrap analysis (<50%) and posterior probabilities (<0.5). Hence, the relationships at this level cannot be established with confi-

dence. However, there is support for the branching pattern of the terminal taxa, and in a few cases, their sister group relationships. With respect to the relationship between the taxa of interest in this study, PhyML analysis suggests the two species of *Palatinus* to be related to *Peridiniopsis borgei*. The relationship between *Palatinus* spp. and *Peridinium cinctum* and *P. willei* seems distant (Fig. 14), even though this is not supported by any of the methods applied here as measure of branch support. Thus, the ML analysis does not propose a phylogenetic relationship (i.e., a most recent common ancestor) between *Palatinus* and *Peridinium* as would be expected considering the potential level of taxonomic resolution provided in this data set.

**Sequence divergence.** Estimates of sequence divergence in percent provide a simple measure of rela-

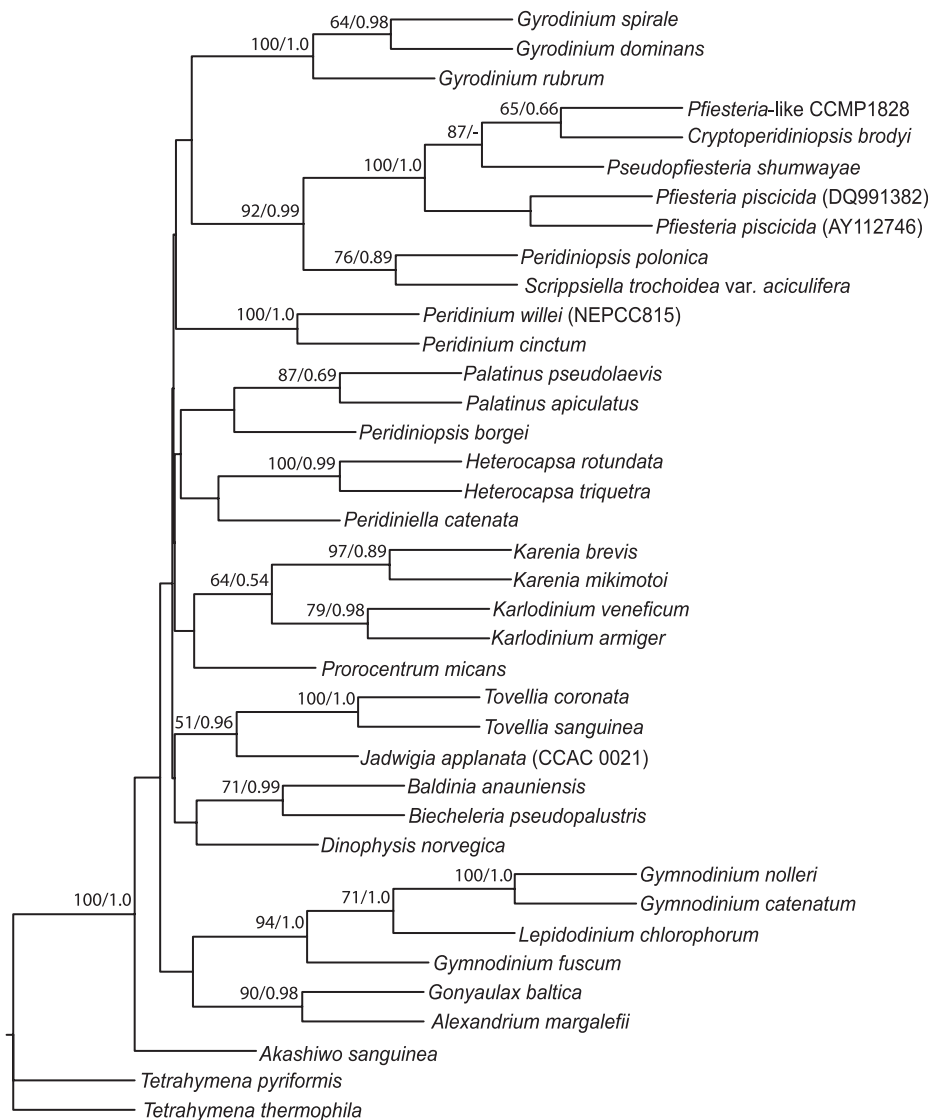


FIG. 14. Phylogenetic tree based on maximum-likelihood (ML) bootstrap analysis (PhyML) of nuclear-encoded LSU rDNA sequences from a diverse assemblage of dinoflagellates including the new genus *Palatinus*. The tree was rooted using two ciliate species of the genus *Tetrahymena*. MrModeltest suggested GTR+G+I as the best-fit nucleotide substitution model and the settings proposed by the program were used in PhyML analysis. Support for nodes was estimated by bootstrap (100 replications in ML) and posterior probabilities in Bayesian analysis. Only bootstrap values  $\geq 50\%$  and posterior probabilities  $\geq 0.5$  are written to the left of nodes. The branch lengths are proportional to the number of character changes.

TABLE 1. Sequence divergence estimates in percent between *Palatinus* spp., *Peridinium* spp., and *Peridiniopsis borgei*. Estimates based on 991 base pairs of the nuclear-encoded LSU rDNA sequences. Uncorrected distances (*P*-values from PAUP\*) are provided above the diagonal, and distance values calculated using the Kimura-2-parameter model are given below the diagonal.

	<i>Palatinus apiculatus</i>	<i>Palatinus pseudolaevis</i>	<i>Peridiniopsis borgei</i>	<i>Peridinium cinctum</i>	<i>Peridinium williei</i>
<i>P. apiculatus</i>	–	6.7	11.5	17.1	19.4
<i>P. pseudolaevis</i>	7.3	–	11.1	17.7	19.7
<i>P. borgei</i>	12.6	12.1	–	19.5	21.4
<i>P. cinctum</i>	19.7	20.5	23.0	–	9.5
<i>P. williei</i>	22.8	23.1	25.8	10.3	–

relationship as similar nucleotide sequences are expected to mirror relatedness. However, in cases of lateral gene transfer, similar sequences will (in most cases) misleadingly suggest a close relationship. Here the sequence divergence estimates for pairwise comparisons between the two species belonging to *Peridinium* and *Palatinus*, respectively, and *Peridiniopsis borgei* are shown in Table 1. Depending on the method used to calculate the sequence divergence, the values between *Palatinus* spp. (6.7%, 7.3%) and *Peridinium* spp. (9.5%, 10.3%) are significantly lower than the values obtained from comparisons between the two genera (17.1%, 19.7% and 19.7%, 23.1%). The sequence divergence estimates between *Palatinus* spp. and *P. borgei* were 11.1%, 11.5% and 12.1%, 12.6%, and considerably higher values were seen when comparing *Peridinium* spp. and *P. borgei* (19.5%, 21.4% and 23.0%, 25.8%). The sequence divergence values in percent given as numbers above are based on uncorrected distances (*P*-values in PAUP\*) and the Kimura-2-parameter model, respectively.

#### DISCUSSION

*Taxonomy and nomenclature of Palatinus species.* The original descriptions of *Peridinium palatinum* and *P. marssonii* display significant similarities between the two species, notably the absence of areolations on the thecal plates, the “wing-like” raised borders of the epithecal plates, and the more or less spiny posterior ends of the cells (Lauterborn 1896, Lemmermann 1900a). However, the lack of illustrations and of defined tabulation patterns rendered the identities of both species uncertain, and the two names were listed in equal standing in a compilation by Lemmermann (1900b). The publication of illustrations and a tabulation formula for *P. marssonii* (Lemmermann 1910, pp. 658, 678), although inaccurate (see below), followed by Schilling’s (1913) inclusion of *P. palatinum* in a list of uncertain species, were probably responsible for the limited use of the latter name during the following years (e.g., Bachmann 1911, Lindemann 1919).

The interpretation of *P. laeve* was facilitated by illustrations and an accurate tabulation scheme, showing the apex of the cell with four plates symmetrically arranged around a square, central plate (Huitfeldt-Kaas 1900). In contrast, the tabulation described for the epitheca of *P. anglicum* was erroneous and misleading, as pointed out by Lindemann (1919, p. 259). The arrangement of the 11 plates recognized in the apical view of *P. anglicum* (West 1909) closely matched the tabulation later described for *P. marssonii* (Lemmermann 1910), except that the plate labeled ventral-apical contacts the precingular plate 6 in *P. anglicum*. Lemmermann’s (1910) statement that the right dorsal-apical plate of *P. marssonii* contacted precingular plate 7 disagrees with the ventral view of the theca included, just as the regular-looking ventral and dorsal views of *P. anglicum* disagree with the interpretation of the tabulation by West (1909, fig. 23C, p. 190) and Lemmermann (1910, p. 679). However, the apical views of the two species given by these authors can easily be matched to the epithecal arrangements of the plates later ascribed to *P. palatinum*, by presuming that the steepness of the ventral side of the theca conceals plates 1’ and 7’’ (compare with Fig. 2d, relabeling plates 2’, 3’, and 4’ as r, va, and 7 pr, respectively).

Lindemann (1919) reviewed the group “*Peridinium-laeve-marssonii-anglicum*” and concluded that features such as a slight difference in the size of the antapical plates and the concavity or convexity of plates, previously used as discriminating characters, were not reliable, and that species distinction could only be based on the tabulation of the epitheca. Although noting the good correspondence between the diagnoses of *P. palatinum* and *P. marssonii*, Lindemann (1919) left *P. palatinum* out of the discussion for lack of figures to clarify its features. All the variant forms in the group were classified in a single species, for which he used the name *P. laeve*, with both *P. marssonii* and *P. anglicum* ranked as subspecies; several variations in plate tabulation, mainly affecting the position of sutures and contacts between plates, were described as varieties, classified mainly in subsp. *marssonii* (Lindemann 1919, 1920).

Lindemann eventually became convinced that *P. palatinum* was conspecific with *P. laeve*, a synonymy previously indicated by Lauterborn (1910, p. 498), and started using the former name (Lindemann 1924, 1925a); his statement that *P. marssonii* was identical to *P. palatinum* was substantiated by the study of samples given to him by Lauterborn (Lindemann 1925b, p. 189). Although Lindemann did not formally recombine the infraspecific taxa previously recognized under *P. laeve* with *P. palatinum*, he did distinguish the asymmetric arrangement of plates around the long, triangular plate 3’ of *P. palatinum* from the symmetric disposition seen at the apex of *P. laeve*, which he named *P. palatinum* f. *laeve* (Huitfeldt-Kaas) Er. Lindemann

(1925a, p. 478, 1925b, p. 189). The high proportion of nearly symmetric cells of strain NIES-1405, analyzed in the present study, in contrast with the regularity of strongly asymmetric cells in the populations examined of *Palatinus apiculatus*, suggests this symmetry to be a stable, inheritable feature and supports the recognition of an independent taxon.

Although Lefèvre (1926) confirmed Lindemann's observations and agreed, in general, with his taxonomic decisions, he also detected a new, unnoticed taxon among the previous illustrations of *P. laeve*-like cells with a symmetric apex. On the basis of observations in fig. 18 in Lindemann (1920, p. 128) and his own study of material collected in Haute-Savoie, French Alps, by Georges Deflandre, Lefèvre (1926, p. 341) described the new species *P. pseudolaeve*, using the markedly striated intercalary bands as a specific character. Although, as shown in Figure 2, a and b, the sutures of *Palatinus apiculatus* are not completely smooth, striations appear rather faint in classical, bright-field LM and are usually not represented in published drawings of the species (Lefèvre 1932, Starmach 1974, Popovský and Pfister 1990); notable exceptions are Skuja (1930, pl. I, figs. 8, 9, as *Peridinium anglicum*) and Wołoszyńska (1952, pl. XVII, figs. 6, 9). The more rounded, less compressed shape, the absence of flanges bordering the epithecal plates, and the lack of strong spines in the hypotheca combine with the distinctly striated sutures and the symmetrical arrangement of the apical plates to make *Palatinus pseudolaevus* a clearly recognizable species.

Lindemann (1928) brought *Glenodinium apiculatum* into the context of this group by noting that both *Peridinium marssonii* and *P. palatinum* were identical to this species, described by Ehrenberg (1838). Without first-hand knowledge of *G. apiculatum*, Stein (1878, p. 92, 1883) had regarded it as a developmental stage of *Peridinium tabulatum* Ehrenb. However, the smooth theca, the raised edges of the epithecal plates, the spiny posterior end of the cells, and the epitheca with the typical twist toward the left, as seen in Ehrenberg's original illustrations (see Fig. 1), all match the current concept of *Peridinium palatinum*, and Lindemann's (1928) proposed synonymy has not been disputed.

Although the name *P. apiculatum* "(Ehrenb.) Er. Lindemann" was used by contemporary authors (Höll 1928, Eddy 1930), Lefèvre (1932) retained *P. palatinum* as the correct name for the species; whether this decision was idiosyncratic or had some nomenclatural basis was not explained. One possible nomenclatural consideration would be that *P. apiculatum* Penard (Penard 1891, p. 51, pl. III, figs. 3–13) would have priority over Lindemann's (1928) combination. However, the original transfer of *Glenodinium apiculatum* to *Peridinium* dates back to Claparède and Lachmann (1859), with the consequence that Penard's *P. apiculatum* is a later homonym, and therefore illegitimate, and Lindemann's

intended new combination *P. apiculatum* is a later isonym, without nomenclatural status (McNeill et al. 2006, Art. 6, Note 2).

Meunier (1919) transferred *G. apiculatum* Ehrenb. to the newly described genus *Properidinium*, erected to receive a diverse assemblage of marine and freshwater species with only 13 epithecal plates. Although arguably illegitimate (it included the type species of *Heterocapsa* F. Stein), the genus was later typified by Loeblich and Loeblich (1966, p. 51), who selected *Properidinium avellana* Meunier as lectotype. Lebour (1925, p. 108) treated *P. avellana* as a species of *Peridinium*, and Balech (1974, p. 54) transferred it to *Protoperidinium* Bergh; the presence of an elongated apical pore complex was documented by Wall and Dale (1968, pl. 4, fig. 1), who obtained thecae from the germination of cysts identical to *Chytrioisphaeridia cariacensis* D. Wall. The cyst was subsequently transferred to *Brigantedinium* P. C. Reid (Reid 1977, p. 434). Fensome et al. (1993) considered *Properidinium* to be a synonym of *Archaeperidinium* Jörgensen, which they assigned, together with *Brigantedinium*, to a family characterized by the presence of only four plates in the cingulum, and with no affinity with the group of species studied herein.

*Morphology and ultrastructure.* Although the arrangement of the chloroplast, with lobes radiating from a central pyrenoid, is a striking feature in axial sections of *Palatinus apiculatus*, it is relatively difficult to perceive in whole cells, probably because the pyrenoid is not enveloped by a layer of starch. Cytoplasmic channels penetrating the pyrenoid matrix are common in several groups of chlorophytes (e.g., Dodge 1973) but have been described in few dinoflagellates; these include species of *Heterocapsa* (Dodge and Crawford 1971, Horiguchi 1995, Tamura et al. 2005) and *Bysmatrum arenicola* Horiguchi et Pienaar (Horiguchi and Pienaar 1988). However, another species with peridinioid affinities, *Peridiniopsis borgei*, has been shown to lack cytoplasmic channels in the pyrenoid (Calado and Moestrup 2002).

The eyespot of *P. apiculatus* belongs to type A sensu Moestrup and Daugbjerg (2007), defined to include eyespots consisting of rows of electron-opaque globules inside a chloroplast lobe located in the sulcal area. Diversity within this type of eyespot includes variation in size and in number of rows of globules, from the relatively small-sized eyespots of, for example, *Peridinium cinctum* and *Baldinia anauniensis*, with a single or two ill-defined rows, to large types as in *Peridiniopsis borgei*, with up to six rows (Calado et al. 1999, Calado and Moestrup 2002, Hansen et al. 2007). In *Palatinus apiculatus*, the eyespot is about as long as in *P. borgei*, although it shows only two longitudinal and the unusual oblique rows of globules. A layer of crystal-like (brick-like) material was found between the eyespot-containing chloroplast lobe and the LMR (r1 flagellar root) of both *P. borgei* and *B. anauniensis*, but not in *P. apiculatus*.

Bacteria are commonly found inside dinoflagellate cells, both in the cytoplasm and, more rarely, in the nucleus (Silva and Franca 1985). Although cultured cells of *P. apiculatus* did not show signs of being harmed by the large numbers of bacteria they contained, their presence did not seem to be required because no bacteria were detected in cells fixed from a field sample. The number of intracellular bacteria had no significant effect on the growth or survival of cultured *Heterocapsa circularisquama* T. Horiguchi (Maki and Imai 2001).

Cytoplasmic vesicles containing bundles of thin fibers are a regular feature of dinoflagellate cells and, following Leadbeater (1971), are generally interpreted as being involved in the formation of flagellar hairs. Figure S1a supports the idea that dictyosomes are involved in the maturation of these fibrillar vesicles (Leadbeater 1971).

Microtubular strands located near the flagellar base area, but not attached to flagellar roots, have been found in most dinoflagellates examined in detail. Dinoflagellates that have such rows of microtubules fall into two groups: the ones with several overlapping rows capable of extending into an external tube commonly used for food uptake, as shown for *Peridiniopsis berolinensis* (Lemmerm.) Bourrelly (Calado and Moestrup 1997), and those with a single row of microtubules, which vary in number from nearly 80 in *Peridiniopsis borgei* (Calado and Moestrup 2002) to about 26 in the small-celled *Prosoaulax lacustris* (F. Stein) Calado et Moestrup (Calado et al. 1998, as *Amphidinium lacustre* F. Stein non auctt.; see Calado and Moestrup 2005). Although it is not clear what function these microtubular strands have in some species, the use of microtubule-driven peduncles for feeding, probably involving the electron-opaque vesicles usually located along the microtubules, is well documented (Hansen and Calado 1999). Judging from its position and orientation, the microtubular strand positioned adjacent to the flagellar base area of *P. apiculatus* is interpreted as homologous to the rows of microtubules involved in peduncle extension in other dinoflagellates. The short length of the microtubules, not reaching the cell surface, the lack of accompanying vesicles, and the absence of a definite exit location for a peduncle, such as a striated collar, suggest that the microtubular strand of *P. apiculatus* is nonfunctional, perhaps an evolutionary leftover.

*Comparison with typical Peridinium.* The genus *Peridinium* is typified by *P. cinctum* (O. F. Müll.) Ehrenb., currently classified in group *cinctum* together with *P. gatunense* Nygaard and *P. raciborskii* Wołosz. Group *willei*, comprising *P. willei* Huitfeldt-Kaas and *P. volzii* Lemmerm., differs from species of group *cinctum* in having the epithelial plates disposed symmetrically relative to the ventral–dorsal axis (Popovský and Pfister 1990). The general appearance of the cells and the tabulation features

are otherwise similar in the two groups, and *P. willei* consistently pairs with *P. cinctum* in DNA-derived phylogenetic schemes (Fig. 14 and, e.g., Calado et al. 2006, Moestrup et al. 2008). The features common to all these species, as far as they are known, therefore represent typical *Peridinium* characters.

*Peridinium* group *palatinum* is separated from other groups of species without an apical pore by the presence of two, rather than three, anterior intercalary plates (e.g., Bourrelly 1970, Popovský and Pfister 1990). As seen in the present work, this correlates with other differences from typical *Peridinium* features. The presence of six cingular plates in *Palatinus*, against five in typical *Peridinium*, would by itself warrant a separate generic status to *Palatinus* species in a widely followed practice initiated by Balech for marine dinoflagellates (Balech 1959). However, given the high number of thecate species for which cingular details had not been reported, Bourrelly (1968, 1970, pp. 52–3) did not adopt the number of cingular plates as a generic level character in his account of the freshwater dinoflagellates. Another notable aspect of the theca of *Palatinus* is the smooth or finely granulate surface of the plates, with no traces of the ridges that form the areolate pattern seen in typical *Peridinium* species (e.g., Hickel and Pollinger 1988, Olrik 1992, Calado et al. 1999).

Cells of *Peridinium* sensu Popovský and Pfister (1990) shed the theca when they divide, and sometimes also without dividing, a process known as ecdysis (e.g., Taylor 1987). The way the theca opens for the exiting cells is quite regular within a species (Lefèvre 1932, p. 21). In *P. cinctum*, *P. willei*, and *P. volzii*, an operculum formed by the dorsal half of the epitheca breaks off, made of plates 3', 1a, 2a, 3a, 3'', 4'', 5'', as reported by Boltovskoy (1973, 1975)—who applied the term archeopyle to the theca rather than to the cyst—and repeatedly confirmed by us (A. Calado and S. Craveiro, unpublished observations). The theca of *P. gatunense* opens along the upper edge of the cingulum (Boltovskoy 1973). In contrast, thecae of *Palatinus* species break open in the antapical area.

The occurrence of cells dividing in an athecate, swimming stage, reported here for dense *P. apiculatus* populations in the Kollelev ponds, was previously described by West (1909, p. 189) from Warwickshire, middle England, who saw in this division mode “the reason for the occurrence of prodigious numbers of active individuals” in Bracebridge Pool, in April. Although this division in the swimming stage seems restricted to rapidly growing, dense populations, and the more common exit of already divided cells from the parent theca may also occur in *P. apiculatus*, it is noteworthy that a similar division strategy has never been reported, even for dense populations of any other species.

The most striking difference between the internal structure of *Palatinus* and typical *Peridinium* is the

connection of peripheral lobes to a central, branching pyrenoid described in the present work, in contrast with the entirely peripheral plastid system reported for *P. cinctum* (Spector and Triemer 1979, Calado et al. 1999) and *P. gatunense* (Messer and Ben-Shaul 1969, as *P. westii* Lemmerm.). Seo and Fritz (2002) documented a diel migration of chloroplasts (or chloroplast lobes) in *P. volzii*, located at the periphery during the dark phase and retreating toward the center of the cell, with the pyrenoid-containing areas inward, during the light phase, but without connecting into a single entity.

Ultrastructural details of typical *Peridinium* species for comparison with *Palatinus apiculatus* are only available from *Peridinium cinctum*. The structure documented in Figure 3, a and c, in the thecal pores of *P. apiculatus* was not found in a detailed study of the theca of *P. cinctum* (Dürr 1979). The well-defined pusular tubes occurring in *P. apiculatus* were not present in *P. cinctum*. In the latter species, numerous irregularly shaped pusular tubes and vesicles were directly linked to the flagellar canals and sac pusules, and abundant profiles of pusular elements were present in the ventral area (Calado et al. 1999). The comparatively more localized pusular system of *P. apiculatus* suggests a different strategy for establishing a large contact area between pusule and cytoplasm, perhaps mainly through the surface of the spreading wrapping vesicles.

*P. cinctum* was found to lack a microtubular strand homologous to those involved in peduncle formation in other dinoflagellates (Calado et al. 1999). In contrast, such a microtubular system was observed in all cells of *P. apiculatus* examined in the present work (see above). The distinct fibers connecting the TB to the dorsal side of the LMR and the aspect of the LC in cross-section, as documented here for *P. apiculatus*, are reminiscent of similar structures in *Peridiniopsis borgei*, which they resemble more than those of *P. cinctum* (Calado and Moestrup 2002). Taken together, these features and the chloroplast organization with a large, central pyrenoid, suggest that *P. apiculatus* has retained more plesiomorphic characters from the common ancestor to *Peridinium* and *Peridiniopsis* than *P. cinctum*.

The molecular phylogeny presented in Figure 14 complements the comparison of morphological features outlined above and also suggests the separation of the two *Palatinus* species from the *P. cinctum* group. Although this molecular phylogenetic indication is weakened by the low bootstrap values and posterior probabilities supporting the branching pattern, the ML analysis did propose a somewhat distant relationship between typical *Peridinium* and a clade comprising *P. borgei* and the *Palatinus* species. Additionally, the sequence divergence estimates indicated that the percentage difference between *Palatinus* and *Peridinium* is in the same range as that seen at the genus level for other dinoflagellates (N.

Daugbjerg, pers. observation). We therefore interpret that the LSU rDNA sequence data provide indirect support to the morphological reasoning for erecting the new genus *Palatinus*. Future gene sequence analyses, preferably of nonribosomal nuclear and mitochondrial genes, should be performed to elucidate further the evolutionary history and phylogeny of *Palatinus* and species belonging to the *P. cinctum* group.

S. C. C. was supported by a Ph.D. fellowship from the financing program POCI, Portugal (SFRH/BD/16794/2004), and by a grant from the European Commission's (FP 6) Integrated Infrastructure Initiative programme SYNTHESIS (DK-TAF) during July–September 2008. Ø. M. gratefully acknowledges a grant from the Villum-Kann Rasmussen Foundation. We thank Ramiro Logares for sending an extracted DNA sample of *Peridiniopsis borgei*.

- Bachmann, H. 1911. *Das Phytoplankton des Süßwassers mit besonderer Berücksichtigung des Vierwaldstättersees*. Gustav Fischer, Jena, Germany, 213 pp., 15 pls.
- Balech, E. 1959. Two new genera of dinoflagellates from California. *Biol. Bull.* 116:195–203.
- Balech, E. 1974. El género "Proto*peridinium*" Bergh, 1881 ("Peridinium" Ehrenberg, 1831, partim). *Rev. Mus. Argent. Cienc. Nat. Hidrobiol.* 4:1–79.
- Bergholtz, T., Daugbjerg, N., Moestrup, Ø. & Fernández-Tejedor, M. 2006. On the identity of *Karlodinium veneficum* and description of *Karlodinium armiger* sp. nov. (Dinophyceae), based on light- and electron microscopy, nuclear-encoded LSU rDNA and pigment composition. *J. Phycol.* 42:170–93.
- Boltovskoy, A. 1973. Formación del arqueopilo en tecas de dinoflagelados. *Rev. Esp. Micropaleontol.* 5:81–98.
- Boltovskoy, A. 1975. Estructura y estereoultraestructura tecal de dinoflagelados. II. *Peridinium cinctum* (Müller) Ehrenberg. *Physis Secc. B* 34:73–84.
- Boltovskoy, A. 1999. The genus *Glochidinium* gen. nov., with two species: *G. penardiforme* comb. nov. and *G. platygaster* sp. nov. (Peridiniaceae). *Grana* 38:98–107.
- Bourrelly, P. 1968. Note sur *Peridiniopsis borgei* Lemm. *Phykos* 7:1–2.
- Bourrelly, P. 1970. *Les algues d'eau douce 3: Les algues bleues et rouges, les Eugléniens, Péridiniens et Cryptomonadines*. Boubée, Paris, 512 pp.
- Calado, A. J., Craveiro, S. C., Daugbjerg, N. & Moestrup, Ø. 2006. Ultrastructure and LSU rDNA-based phylogeny of *Esoprodinium gemma* (Dinophyceae), with notes on feeding behavior and the description of the flagellar base area of a planozygote. *J. Phycol.* 42:434–52.
- Calado, A. J., Craveiro, S. C. & Moestrup, Ø. 1998. Taxonomy and ultrastructure of a freshwater, heterotrophic *Amphidinium* (Dinophyceae) that feeds on unicellular protists. *J. Phycol.* 34:536–54.
- Calado, A. J., Hansen, G. & Moestrup, Ø. 1999. Architecture of the flagellar apparatus and related structures in the type species of *Peridinium*, *P. cinctum* (Dinophyceae). *Eur. J. Phycol.* 34:179–91.
- Calado, A. J. & Moestrup, Ø. 1997. Feeding in *Peridiniopsis berolinensis* (Dinophyceae): new observations on tube feeding by an omnivorous, heterotrophic dinoflagellate. *Phycologia* 36:47–59.
- Calado, A. J. & Moestrup, Ø. 2002. Ultrastructural study of the type species of *Peridiniopsis*, *Peridiniopsis borgei* (Dinophyceae), with special reference to the peduncle and flagellar apparatus. *Phycologia* 41:567–84.
- Calado, A. J. & Moestrup, Ø. 2005. On the freshwater dinoflagellates presently included in the genus *Amphidinium*, with a description of *Prosoaulax* gen. nov. *Phycologia* 44:112–9.
- Claparède, E. & Lachmann, J. 1859. Études sur les Infusoires et les Rhizopodes. *Mém. Inst. Natl. Geneve* 6:261–482, pls. 14–24.
- Daugbjerg, N., Hansen, G., Larsen, J. & Moestrup, Ø. 2000. Phylogeny of some of the major genera of dinoflagellates based on

- ultrastructure and partial LSU rDNA sequence data, including the erection of three new genera of unarmoured dinoflagellates. *Phycologia* 39:302–17.
- De Rijk, P., Wuyts, J., van der Peer, Y., Winkelmann, T. & Wachter, R. 2000. The European large subunit ribosomal RNA database. *Nucleic Acids Res.* 28:117–8.
- Dodge, J. D. 1973. *The Fine Structure of Algal Cells*. Academic Press, London, xii + 261 pp.
- Dodge, J. D. & Crawford, R. M. 1971. A fine-structural survey of dinoflagellate pyrenoids and food-reserves. *Bot. J. Linn. Soc.* 64:105–15.
- Dürr, G. 1979. Elektronenmikroskopische Untersuchungen am Panzer von Dinoflagellaten. II. *Peridinium cinctum*. *Arch. Protistenkd.* 122:88–120.
- Eddy, S. 1930. The fresh-water armored or thecate dinoflagellates. *Trans. Am. Microsc. Soc.* 49:277–321.
- Ehrenberg, C. G. 1838. *Die Infusionsthierehen als vollkommene Organismen. Ein Blick in das tiefere organische Leben der Natur*. Leopold Voss, Leipzig, Germany, 547 pp., 64 pls.
- Felsenstein, J. 2008. *Phylogeny Inference Package (PHYLIP)*. Version 3.68. University of Washington, Seattle. <http://evolution.genetics.washington.edu/phylip.html> (last accessed 17 June 2009).
- Fensome, R. A., Taylor, F. J. R., Norris, G., Sarjeant, W. A. S., Wharton, D. I. & Williams, G. L. 1993. A classification of living and fossil dinoflagellates. *Micropaleontology*, Special Publication Number 7, 351 pp.
- Guindon, S. & Gascuel, O. 2003. PhyML – a simple, fast, and accurate algorithm to estimate large phylogenies by maximum likelihood. *Syst. Biol.* 52:696–704.
- Hansen, P. J. & Calado, A. J. 1999. Phagotrophic mechanisms and prey selection in free-living dinoflagellates. *J. Eukaryot. Microbiol.* 46:382–9.
- Hansen, G. & Daugbjerg, N. 2004. Ultrastructure of *Gyrodinium spirale*, the type species of *Gyrodinium* (Dinophyceae), including a phylogeny of *G. dominans*, *G. rubrum* and *G. spirale* deduced from partial LSU rDNA sequences. *Protist* 155:271–94.
- Hansen, G., Daugbjerg, N. & Henriksen, P. 2000. Comparative study of *Gymnodinium mikimotoi* and *Gymnodinium aureolum* comb. nov. (= *Gyrodinium aureolum*) based on morphology, pigment composition, and molecular data. *J. Phycol.* 36:394–410.
- Hansen, G., Daugbjerg, N. & Henriksen, P. 2007. *Baldinia anaunensis* gen. et sp. nov.: a 'new' dinoflagellate from Lake Tovel, N. Italy. *Phycologia* 46:86–108.
- Hansen, G. & Flaim, G. 2007. Dinoflagellates of the Trentino Province, Italy. *J. Limnol.* 66:107–41.
- Hickel, B. & Pollinger, U. 1988. Identification of the bloom-forming *Peridinium* from lake Kinneret (Israel) as *P. gatunense* (Dinophyceae). *Br. Phycol. J.* 23:115–9.
- Höll, K. 1928. Oekologie der Peridineen. Studien über den Einfluß chemischer und physikalischer Faktoren auf die Verbreitung der Dinoflagellaten im Süßwasser. *Pflanzenforschung* 11:I–VI. 1–105.
- Horiguchi, T. 1995. *Heterocapsa circularisquama* sp. nov. (Peridinales, Dinophyceae): a new marine dinoflagellate causing mass mortality of bivalves in Japan. *Phycol. Res.* 43:129–36.
- Horiguchi, T. & Pienaar, R. N. 1988. Ultrastructure of a new sand-dwelling dinoflagellate, *Scrippsiella arenicola* sp. nov. *J. Phycol.* 24:426–38.
- Huber-Pestalozzi, G. 1950. Cryptophyceen, Chloromonaden, Peridineen. In Thienemann, A. [Ed.] *Die Binnengewässer*, vol. 16. E. Schweizerbart'sche Verlagsbuchhandlung, Stuttgart, Germany, 310 pp.
- Huitfeldt-Kaas, H. 1900. Die limnetischen Peridineen in norwegischen Binnenseen. *Vid. Selsk. Skr. [Christiania] Math. Naturv. Kl.* 2:1–7, 1 pl.
- Imamura, K. & Fukuyo, Y. 1990. *Peridinium penardiforme* Lindemann. In Fukuyo, Y., Takano, H., Chihara, M. & Matsuoka, K. [Eds.] *Red Tide Organisms in Japan – An Illustrated Taxonomic Guide*. Uchida Rokakuho, Tokyo, pp. 52–3.
- Kiselev, I. A. 1954. Pirofitovye vodorosli. In Gollerbakh, M. M. & Polianskii, V. I. [Eds.] *Opredelitel' presnovodnykh vodoroslei SSSR*, vol. 6. Sovetskaya Nauka, Moskva, p. 212.
- Lauterborn, R. 1896. Diagnosen neuer Protozoen aus dem Gebiete des Oberrheins. *Zool. Anz.* 19:14–8.
- Lauterborn, R. 1910. Die Vegetation des Oberrheins. *Verh. Naturh. Med. Ver. Heidelberg N.F.* 10:450–502.
- Leadbeater, B. S. C. 1971. The intracellular origin of flagellar hairs in the dinoflagellate *Woloszynskia micra* Leadbeater & Dodge. *J. Cell Sci.* 9:443–51.
- Lebour, M. V. 1925. *The Dinoflagellates of Northern Seas*. Marine Biological Association of the United Kingdom, Plymouth, UK, vii + 250 pp.
- Lefèvre, M. 1926. ('1925') Contribution à la flore des Péridiniens de France. *Rev. Algol.* 2:327–42, pls. XI–XII.
- Lefèvre, M. 1932. Monographie des espèces d'eau douce du genre *Peridinium*. *Arch. Bot.* 2(Mémoire 5):1–210.
- Lemmermann, E. 1900a. Beiträge zur Kenntniss der Planktonalgen. III. Neue Schwebalgen aus der Umgegend von Berlin. *Ber. Deutsch. Bot. Ges.* 18:24–32.
- Lemmermann, E. 1900b. Beiträge zur Kenntniss der Planktonalgen. VIII. Peridinales aquae dulcis et submarinae. *Hedwigia* 39:115–21.
- Lemmermann, E. 1910. *Kryptogamenflora der Mark Brandenburg. Bd. 3. Algen I (Schizophyceen, Flagellaten, Peridinee)*. Gebrüder Borntraeger, Leipzig, Germany, 712 pp.
- Lewis, C. T. & Short, C. 1879. *A Latin Dictionary Founded on Andrews' Edition of Freund's Latin Dictionary*. Oxford University Press, Oxford, UK, xiv + 2019 pp.
- Lindemann, E. 1919. Untersuchungen über Süßwasserperidinee und ihre Variationsformen. *Arch. Protistenk.* 39:209–62, pl. 17.
- Lindemann, E. 1920. Untersuchungen über Süßwasserperidinee und ihre Variationsformen II. *Arch. Naturg. Sec. A* 84:121–94.
- Lindemann, E. 1924. Peridineen des Alpenrandgebietes. *Bot. Arch.* 8:297–303.
- Lindemann, E. 1925a. Peridineen des Oberrheins und seiner Altwässer. *Bot. Arch.* 11:474–81.
- Lindemann, E. 1925b. III. Klasse: Dinoflagellatae (Peridinee). In Schoenichen, W. [Ed.] *[Eyferth's] Einfachste Lebensformen des Tier- und Pflanzenreiches*, 5th ed., vol. 1, Spaltpflanzen, Geißelalgen, Algen, Pilze. Hugo Bermühler Verlag, Berlin-Lichterfelde, Germany, pp. 144–95.
- Lindemann, E. 1928. Vorläufige Mitteilung. *Arch. Protistenk.* 63:259–60.
- Lindström, K. 1991. Nutrient requirements of the dinoflagellate *Peridinium gatunense*. *J. Phycol.* 27:207–19.
- Loeblich Jr., A. R. & Loeblich III, A. R. 1966. Index to the genera, subgenera, and sections of the Pyrrhophyta. *Stud. Trop. Oceanogr.* 3:i–ix, 1–94.
- Maddison, D. R. & Maddison, W. P. 2003. *MacClade 4*. Sinauer Associates Inc., Publishers, Sunderland, Massachusetts.
- Maki, T. & Imai, I. 2001. Relationships between intracellular bacteria and the bivalve killer dinoflagellate *Heterocapsa circularisquama* (Dinophyceae). *Fish. Sci.* 67:794–803.
- McNeill, J., Barrie, F. R., Burdet, H. M., Demoulin, V., Hawksworth, D. L., Marhold, K., Nicolson, D. H., et al. [Eds.] 2006. *International Code of Botanical Nomenclature (Vienna Code)*, Adopted by the Seventeenth International Botanical Congress, Vienna, Austria, July 2005. A.R.G. Gantner Verlag, Ruggell, Liechtenstein, xviii + 568 pp. (*Regnum Vegetabile* 146).
- Messer, G. & Ben-Shaul, Y. 1969. Fine structure of *Peridinium westii* Lemm., a freshwater dinoflagellate. *J. Protozool.* 16:272–80.
- Meunier, A. 1919. Microplankton de la Mer Flamande. 3<sup>me</sup> Partie. Les Péridiniens. *Mém. Mus. R. Hist. Nat. Belg.* 8:1–116, pls. 15–21.
- Moestrup, Ø. 2000. The flagellate cytoskeleton. Introduction of a general terminology for microtubular flagellar roots in protists. In Leadbeater, B. S. C. & Green, J. C. [Eds.] *The Flagellates. Unity, Diversity and Evolution*. Taylor & Francis, New York, pp. 69–94 (Systematics Association Special Volume No. 59).
- Moestrup, Ø. & Daugbjerg, N. 2007. On dinoflagellate phylogeny and classification. In Brodie, J. & Lewis, J. [Eds.] *Unravelling the Algae: The Past, Present, and Future of Algal Systematics*. CRC

- Press, Boca Raton, Florida, pp. 215–30 (Systematics Association Special Volume No. 75).
- Moestrup, Ø., Hansen, G. & Daugbjerg, N. 2008. Studies on woloszynskioid dinoflagellates III: on the ultrastructure and phylogeny of *Borghiella dodgei* gen. et sp. nov., a cold-water species from Lake Tovel, N. Italy, and on *B. tenuissima* comb. nov. (syn. *Woloszynskia tenuissima*). *Phycologia* 47:54–78.
- Moestrup, Ø., Hansen, G., Daugbjerg, N., Flaim, G. & d'Andrea, M. 2006. Studies on woloszynskioid dinoflagellates II: on *Tovellia sanguinea* sp. nov., the dinoflagellate responsible for the reddening of Lake Tovel, N. Italy. *Eur. J. Phycol.* 41:47–65.
- Nylander, J. A. A. 2004. *MrModeltest v2*. Program distributed by the author. Evolutionary Biology Centre, Uppsala University, Uppsala, Sweden.
- Olrik, K. 1992. Ecology of *Peridinium willei* and *P. volzii* (Dinophyceae) in Danish lakes. *Nord. J. Bot.* 12:557–68.
- van de Peer, Y., van der Auwera, G. & De Wachter, R. 1996. The evolution of stramenopiles and alveolates as derived by “substitution rate calibration” of small ribosomal subunit RNA. *J. Mol. Evol.* 42:201–10.
- Penard, E. 1891. Les Péridiniacées du Léman. *Bull. Trav. Soc. Bot. Genève* 6:1–63, pls. I–V.
- Popovský, J. & Pfister, L. A. 1990. Dinophyceae (Dinoflagellida). In Ettl, H., Gerloff, J., Heynig, H. & Mollenhauer, D. [Eds.] *Süßwasserflora von Mitteleuropa*, vol. 6. Gustav Fischer, Jena, Germany, 272 pp.
- Reid, P. C. 1977. Peridiniacean and glenodiniacean dinoflagellate cysts from the British Isles. *Nova Hedwigia* 29:429–63.
- Ronquist, F. & Huelsenbeck, J. P. 2003. MRBAYES 3: Bayesian phylogenetic inference under mixed models. *Bioinformatics* 19:1572–4.
- Schiller, J. 1937. Dinoflagellatae (Peridineeae) in monographischer Behandlung. In Kolkwitz, R. [Ed.] *Rabenhorst's Kryptogamenflora von Deutschland, Österreich und der Schweiz*, 2nd ed., vol. 10 (3). Part 2. Akademische Verlagsgesellschaft, Leipzig, Germany, 589 pp.
- Schilling, A. J. 1913. Dinoflagellatae (Peridineeae). In Pascher, A. [Ed.] *Süßwasser-Flora Deutschlands, Österreichs und der Schweiz*, vol. 3. Gustav Fischer, Jena, Germany, 66 pp.
- Seo, K. S. & Fritz, L. 2002. Diel changes in pyrenoid and starch reserves in dinoflagellates. *Phycologia* 41:22–8.
- Silva, E. S. & Franca, S. 1985. The association dinoflagellate-bacteria: their ultrastructural relationship in two species of dinoflagellates. *Protistologica* 21:429–46.
- Skuja, H. 1930. ('1929') Süßwasseralgae von den westestnischen Inseln Saaremaa und Hiiumaa. *Acta Hort. Bot. Univ. Latv.* 4: 1–76, pls. I–III.
- Spector, D. L. & Triemer, R. E. 1979. Ultrastructure of the dinoflagellate *Peridinium cinctum* f. *ovoplanum*. I. Vegetative cell ultrastructure. *Am. J. Bot.* 66:845–50.
- Starmach, K. 1974. Cryptophyceae, Dinophyceae, Raphidophyceae. In Starmach, K. & Siemińska, J. [Eds.] *Flora Stodkowodna Polski*, vol. 4. Państwowe Wydawnictwo Naukowe, Warszawa, 520 pp.
- Stein, F. 1878. *Der Organismus der Infusionsthiere nach eigenen Forschungen in systematischer Reihenfolge bearbeitet. III. Abtheilung. Die Naturgeschichte der Flagellaten oder Geisselinfusorien. I. Hälfte. Den noch nicht Abgeschlossenen allgemeinen Theil nebst Erklärung der sämtlichen Abbildungen enthaltend.* Wilhelm Engelmann, Leipzig, Germany, 154 pp., 24 pls.
- Stein, F. 1883. *Der Organismus der Infusionsthiere... III. Abtheilung. II. Hälfte. Die Naturgeschichte der arthrodelen Flagellaten. Einleitung und Erklärung der Abbildungen.* Wilhelm Engelmann, Leipzig, Germany, 30 pp., 25 pls.
- Swofford, D. L. 2003. *PAUP\* Phylogenetic Analysis Using Parsimony (\*and Other Methods), version 4*. Sinauer Associates, Sunderland, Massachusetts.
- Tamura, M., Iwataki, M. & Horiguchi, T. 2005. *Heterocapsa psammophila* sp. nov. (Peridinales, Dinophyceae), a new sand-dwelling marine dinoflagellate. *Phycol. Res.* 53:303–11.
- Taylor, F. J. R. 1987. Dinoflagellate morphology. In Taylor, F. J. R. [Ed.] *The Biology of Dinoflagellates*. Botanical Monographs Volume 21. Blackwell Scientific Publ., Oxford, UK, pp. 24–91.
- Wall, D. & Dale, B. 1968. Modern dinoflagellate cysts and evolution of the Peridinales. *Micropaleontology* 14:265–304.
- West, G. S. 1909. A biological investigation of the Peridinieae of Sutton Park, Warwickshire. *New Phytol.* 8:181–96.
- Wilgenbusch, J. C., Warren, D. L. & Swofford, D. L. 2004. AWTY: a system for graphical exploration of MCMC convergence in Bayesian phylogenetic inference. <http://ceb.csit.fsu.edu/awty> (last accessed 17 June 2009).
- Wolozynska, J. 1952. Bruzdnice Tatr i Karpat Wschodnich (Peridynieae montium Tatrensium et Carpathorum Orientalium). *Acta Soc. Bot. Pol.* 21:311–6, pls. I–XVII.

### Supplementary Material

The following supplementary material is available for this article:

**Figure S1.** *Palatinus apiculatus*, ultrastructure. (a) Fibrillar vesicle adjacent to a dictyosome, apparently receiving dictyosome-derived vesicles. (b) Overview of the nucleus (N) with a group of bacteria (b) adjacent to the nucleolus (nu). (c) Detail of an intranuclear bacterium located between the nucleolus and the nuclear envelope. The arrowhead points to a nuclear pore. D, dictyosome.

**Figure S2.** *Palatinus apiculatus*, flagellar apparatus. Nonadjacent serial sections proceeding from left to right, viewed from the cell's left. Small slanted numbers refer to the section number. (a–d) Two pusular tubes connect to the transverse flagellar canal (TFC). The transverse microtubular root (TMR) and its microtubular extension (TMRE) are visible at this level, both encircling the TFC. A strand of microtubules, marked with arrowheads, is seen in (b), adjacent to an accumulation body (ab), and continues in (d–e). Note the left (distal) end of the transverse striated root (TSR) near the transverse striated collar (TSC). LMR, longitudinal microtubular root.

**Table S1.** Alphabetical list of dinoflagellates included in the phylogenetic analyses. The ciliates comprising the outgroup are included below. GenBank accession numbers for the nuclear-encoded LSU rDNA sequences are given for each species.

This material is available as part of the online article.

Please note: Wiley-Blackwell are not responsible for the content or functionality of any supporting materials supplied by the authors. Any queries (other than missing material) should be directed to the corresponding author for the article.